Rock Mechanical Investigation of Clay and Clayey Gouge at High Pressures and Temperatures

Chi-yuen Wang

University of California, Berkeley
Department of Geology and Geophysics
Berkeley, California 94720

USGS CONTRACT NO. 14-08-0001-17747
Supported by the EARTHQUAKE HAZARDS REDUCTION PROGRAM

OPEN-FILE NO. 81-94

Rock Mechanical Investigation of Clay and Clayey Gouge at High Pressures and Temperatures

by Chi-yuen Wang
University of California, Berkeley
Department of Geology and Geophysics
Berkeley, California 94720

FINAL REPORT

Contract No. 14-08-0001-17747

submitted April 25, 1980

FAULT ZONES, GOUGE AND MECHANICAL PROPERTIES OF CLAYS UNDER HIGH PRESSURE

Chi-Yuen Wang

ABSTRACT

Clay minerals are found to be a significant component of all the fault zones, young or old, at surface or at depth down to 2 kilometers. These clays are stable up to 200 to 400 degrees under 1-4 kb of confining pressure. Thus, there are reasons to believe that in the part of the fault zone which earthquakes are found to occur we may encounter clay gouge.

Mechically, the clays are quite weak compared either to rocks or to frictional contacts of rocks. The peak strength under 1-4 kb confining pressure of montmorillonite, a common gouge mineral, is 0.25 to 0.35 kb; its residual strength is 10-20% lower.

INTRODUCTION

Not being able to observe an active fault at the whole depth range, we have to use a combination of methods to decipher the possible types of materials in the fault zones of interest; such information is necessary for the understanding of the mechanics of faulting. The methods at our disposal to investigate the fault zone materials are the same ones used by geologists and geophysicists to learn about the interior of the earth, taking into consideration that the temperature; the amount of fluid circulation, the presence of shear stress, the mechanical communication actions, etc. are factors peculiar to fault zones.

Available to direct observation are outcrops of fault zones of different ages (the time since a fault ceases to be active), types, total displacement, in different country rocks, and in different stagers of denudation. By surface or

stresses; whatever exists at depth, should also be able to reproduce these behaviors and should have strengths that are consistent with the estimated tectonic stresses available to generate earthquakes.

Knowledge of active fault zones can also be augmented by observing at surface, in deep tunnels or drill holes, fault zones that have ceased to be active and has since been uplifted and eroded so that they are now exposed. These fault zones are especially useful in knowing what might exist beyond the depth at which the shallow mineralogy in active fault zone are in equilibrium. A different sort of interpretation problem is involved here. For example, during the long period of quiescence, the fault zone is subjected to the lithostatic stress with little or no shear stress; thus the zone is under "consolidation", the water would have diffused out from the fault zone, carrying with it some of the more mobile ions; it is also possible that if the gouge was in a saturated state, its mobility may result in the depletion of gouge with respect to the breccia. The post faulting burial may also lead to prograde metamorphism. For mylonites that were generated at depth where metamorphism takes place, it would be necessary to know what changes the original fault rocks had gone through in order to reconstruct the fault zone. It is obvious the older fault zones can be used as analogues to the active fault zones after the extraneous factors are removed.

In this paper, we shall first describe the mineralogy and macroscopic appearances of fault zones of several ages that we have studied so far, discuss the stability field of the various clay minerals detected in the fault zone, report on the initial results of triaxial mechanical experiments on whole clay samples and finally make a conjecture on the processes involved in fault zones, their formation, the subsequent actions and the generation of earthquakes. Obviously, we are only dealing with fault zones at the depth range of 0 to about 12 km, beyond which cataclastics may be replaced by mylonites and flow may be the dominant mode of deformation (e.g., Sibson, 1977).

FIELD OBSERVATION AND SAMPLING OF FAULT ZONES

Fault zones in three areas of quite different ages, and in different tectonic settings are studied with respect to their mineralogical compositions and mode of deformation. (1) The two normal faults in southeastern Adirondacks were probably active in late Paleozoic (Fisher et al., 1971) with Pre-Cambrian metamorphic rocks, anorthosites and Paleozoic dolomite in the vicinity. The deformations in these fault zones are in the brittle range; cataclasis is prominantly seen but neomineralization in the fault zone is an important aspect. (2) Several normal and strike-slip faults are encountered in the silver-lead-zinc mines of the Coeur d'Aleue district of northern Idaho (Hobbs et al., 1965). These faults were probably active during Cretaceous to early Tertiary; many of these faults form the fracture systems that control the placement of mineral veins. (3) In the San Andreas system, we have already described the fault gouge mineralogy of several surface outcrop (Wu et al., 1975; Wu, 1978), here we are examining the fault geometry, the mineralogy of several down-hole samples (down to 428 meters) in Dry Valley, California, the mineralogy in one outcrop in southern California that has not been described before and some reflection data across San Andreas.

I. TWO NORMAL FAULTS IN SOUTHEASTERN ADIRONDACKS, NY

Figure 1 shows the location of these fault zones and the geology of the immediate vicinity. The total displacements along these faults are not well known; they are probably in the range of five hundred meters to a few kilometers.

1) The Schroon River fault. This fault has a mapped length of over fifteen kilometers. An easily accessible and good exposure is seen on highway 9 in Warrensburg. The fault zone there has a width of about 20 meters with a "meta-anorthosite" and a "granitic charnockitic gneiss" on the west and the east sides of the fault zone, respectively.

Within a few tens of meters of the boundaries of the fault zone, it is clear that the density of joints is higher than farther out, and the orientations of the joints become quite varied. Some of the joints near the fault zone have irregular surfaces and are filled with a fine-grained greenish gouge. The gouge were evidently not generated in the joints, as the surfaces are still quite intact, with slickensides on fresh rock. The presence of the slicdensides in the gouge and on the joint surfaces indicate that movements along the joints have taken place.

Going into the fault zone, we see breccias of various sites; some of them are still quite angular, although they seem to have undergone substantial rotation and translation. The breccia are surrounded by gouge (Figure 2). It is quite evident that the gouge was not generated by grinding up these angular breccia, rather the angular breccia may have been plucked off from the wall and mixed in with gouge. The breccia are mainly gneissic ones; meta-anorthosite breccia are rarely seen.

The original mineralogy of the wall rocks and the production of alteration in the fault zone are summarized in Table 1. Figure 3a shows an example of unaltered gneiss. Figure 3b shows the result of alteration of the ferromagnesium minerals; the long grains and chlorite streaks seem to be aligned parallel to the horizontal axis of the picture -- the chlorite seems to have healed a sheared rock. Figure 3c shows a sample of what appears in hand specimen as dark green "gouge"; here chlorite dominates and a definite flow texture is obvious.

2) The I-87 fault. This fault also has a mapped length exceeding 15 kilometers. An excellent outcrop is seen along highway I-87 in southeastern Adirondacks (Figure 1). The width of the fault zone is about 30 meters. Here the Ordovician Little Falls dolomite and a Pre-Cambrian metagranite are on the west and east side of the fault zone, respectively.

The metagranite is very similar to the granitic gneiss at the last site (Table 1), and the alteration products are essentially the same. The dolomite breccia is limited to within a few meters of the western boundary of the zone. The fairly angular dolomite breccia is embedded in a fine grained matrix -- showing no sign of having undergone cataclasis in hand specimen -- that is composed of dolomite, quartz and feldspar (Figure 4). Dolomite grains in the matrix seem to fill in all the spaces around the quartz and feldspar grains.

In one part ofthe fault zone, angular breccia of metagranites from apparently different points of the fault wall (different color, grain size and texture) are next to each other with a small amount of gouge among them to fill in the space. The breccia have not been rounded much. It appears as though the gouge, relatively incompetent had carried them about in the fault zone for some distance without rounding the breccia and much of the gouge had subsequently been squeezed out of the system.

DISCUSSION

In the fault zone alteration process a large amount of chlorite is produced. This implies that a good amount of water has to be added to the system to produce them. This presence of ample water can conceivably cause low effective stress in the fault zone. Since the chlorite-rich "gouge" is quite pervasive, they could control the behavior of faulting after the fault zone is formed. Whether chlorite was the mineral in the gouge at the time of activity or is it the result of alteration after the fault had ceased to be active cannot be determined.

II. FAULTS IN DEEP MINES OF NORTHERN IDAHO

Hobbs et al. (1965) have mapped in some detail the faults in Coeur d'Aleue district of northern Idaho (Figure 5). The main fault of the region, the Osburn fault, is a right-lateral strike-slip fault that trends approximately N 70° W and has an estimated total displacement of 25 kilometers. The width of the fault in surface and mine exposure ranges from about 30 meters to 270 meters (Hobbs et al., ibid.). During the Summer of 1978, we could gain access to only one closely timbered tunnel across the Osburn fault; many previously open tunnels across the fault have been damaged due to squeezing ground. Sampling has been carried out across the Osburn as well as a number of smaller faults ranging from less than a meter to about 10 meters in width. The clay mineral contents of the wall rock, breccia and the gouge have been determined. In the sampling process, we have also observed the variations in the fault zone geometry and the internal structures.

A. Fault zone geometry and internal structures.

Exposures of a fault at different depths along the dip and sometimes at several points along the strike allow us to see the fault in three dimensions. It is quite noticeable that the fault surfaces are seldom flat planes; the width may increase or decrease by a factor of 2 over a distance of a few fault widths. All the faults that we can observe (Table 2) in detail are relatively small (1-10 meters) and bounded by quartzite or argillite; the general features are quite similar; they include (1) sheared zone, (2) detached blocks, (3) tightly folded alternating layers of gouge and often crumbly quartzite or argillite, and (4) large lens of gouge. Figure 6 shows the Polaris fault zone at three levels in the Galena Mine. The zones are usually quite wet and the gouge is soft and easily deformed in hand.

B. Clay mineralogy of the wall rock and fault zone materials.

Table 2 lists the fault zone, sample descriptions and mineralogy of the less than 2 microns fraction.

The gouge samples contain chlorite and illite in all cases; these are actually the dominant minerals of the Belt series rocks of this region, and although the relative amounts of these minerals in the Belt series vary considerably, often the gouge is found to be relatively richer in chlorite. Of more interest is the presence of smectites, the expandable clays, in several fault zones. The wall rocks are completely free of such minerals in most cases.

III. SAN ANDREAS FAULT ZONE

Detailed maps in the San Andreas fault zone often reveal that the zone is variable in width. As shown in Figure 7, the faults on the two sides of a valley are sometimes parallel but more often than not curved or seemingly composed of segments. The section from Pearblossom to San Bernardino, however, shows a number of branches nearby. But as these are surface observations, we are by no means certain that the configuration of the fault zone at depth will correspond to that suggested by the surface trace. It is interesting to observe however, the curvature of the bounding faults seem to be related to topography; in the Point Reyes section, the divergent faults at two ends of the Olema Valley are perhaps the cause for the formation of topography lows there. Also, a COCORP seismic reflection profile across the San Andreas fault zone hear Parkfield indicate that the fault zone at depth is about 2 kilometers wide coinciding with the width defined by the surface trace of the two faults.

The gouge in the San Andreas fault zone has been studied previously (Wu et al., 1975; Wu, 1978). Clay mineral assemblages somewhat different from those in Idaho have been found in this zone. It is quite often thought that along the "great bend" of the San Andreas in southern California, there is little clay gouge (e.g., Anderson and Osborne, 1978). The lack of extensive gouge materials in some sections may be due to the predominance of thrust motion there; it could easily be seen that at the surface outcrop of a young thrust, the front is progressively advanced; the hanging wall will break up but no gouge is generated there. As shown in a tunnel crossing the Sierra Madre fault, a thrust, northeast of Los Angeles, the fault zone broadens at depths and substantial amount of intrafault materials, not unlike those seen in the deep mines of Idaho, are found (Proctor, 1970). West of Lake Elizabeth in the west part of the "great bend", a very substantial fault zone is exposed. It consists of severaly brecciated granite, altered in most cases, with gouge in fractures and also as quite massive lens. The outcrop is extensive enough to create a badland topography there. The gouge is found to be composed mainly of montmorillonite and some illite and chlorite (Table 3).

A recent drill hole in Dry Valley just inside the San Andreas fault zone at depths down to 280 meters. The side-wall samples are all clayey in appearance. Their densities, general description and less than 2 microns compositions are shown in Table 4. The mineralogy is not radically different from that in the surface crops of San Andreas or Hayward fault (Wu, 1978). The apparent decrease of montmorillonite with increasing depth is most probably not related to the stability of this mineral, but due to the change of the pH of the solution (see next section).

The COCORP seismic reflection profile mentioned above indicate that the fault zone extends all the way through Moho, at a depth of 25 to 30 km; while the zone above 12 kilometers shows chaotic reflections, the zone below that level is more seismically transparent, i.e., more homogeneous (Long et al., 1979). Other seismic profiles of San Andreas under the Pacific north of Point Arena, California, also indicate a width of about 2 km to a depth of at least 4 km.

CLAY MINERAL STABILITY AT DEPTHS

The T, P stability range for each important clay mineral group is discussed below. Primary emphasis is placed on experimental data, although evidence from field studies is also incorporated into the discussion where appropriate. Special attention should be called to the importance of the extensiveness of Velde's experimental studies and to his important review of the literature in this field (Velde, 1977). It should be remarked here that the stability field of different minerals at the same temperature and pressure is controlled by the pH values (Roberson and Wu, in preparation, 1979).

Kaolinite

Several investigators (Perry and Hower, 1970; Muffler and White, 1969 ; Dunoyer de Segonzac, 1965) have observed the disappearance of Kaolinite with depth. Upper stability temperatures can vary widely from 100°C to over 200°C . Several reasons have been suggested to account for the disappearance of Kaolinite with depth including combination with Mg (Muffler and White, 1965), reaction with other phases to form illite and chlorite (Velde, 1969), or reaction with quartz to produce pyrophyllite.

Kaolinite has also been observed as a common constituent of hydrothermal deposits which have been interpreted to have formed at depths of several kilometers (Keller, 1963; Keller and Hanson, 1968; Lowell and Guilbert, 1970).

Kaolinite, a common constituent of many soil types, appears to be thermally stable from 25°C, 1 atm, to 100° to 250°C (+) at 1-2 kb. Its upper stability is primarily related to the chemistry of the host rock and reacting pore solution. Velde (1977) has pointed out that kaolinite, during epi-metamorphism, is incorporated into other phases due to a displacement of the bulk composition of the silicate system in which it is found, either through an increase in total R^{+} ion content due to chemical reduction of ferric ion or by the increase in availability of R^{+2}

ion to the silicate minerals through the destabilization after dolomite. Furthermore, Velde has stated that the existence of kaolinite in a mineral assemblage will not generally indicate the important factors of silicate equilibria, that is, the ultimate stabilities of the clays present.

Illite

Illite (defined herein as a dioctahedral, aluminous, clay size mica) is reported to be the most abundant clay mineral in argillaceous sedimentary rocks (Grim, 1968). Studies of deeply buried sediments (Dunozer de Segonzac, 1965; Perry and Hower, 1970; Weaver and Beck, 1971) indicate that illite contents increase with increasing temperatures and pressures. Experimental studies of the muscovite-pyrophyllite system by Velde (1969) show that an illite-like phase is stable to temperatures over 400°C at 2 kb pressure. Muscovite, according to Velde (1969), can persist up to over 400°C at 2 kb pressure.

Chlorite

Chlorite is a common constituent of argillaceous sediments. Chlorite and illite are dominant clays reported in rocks of Paleozoic age. Authigenic chlorites formed at relatively low temperatures have been extensively studied by Hayes (1970). Chlorites are also found in deeply buried sedimentary rocks as well as in low-grade metamorphic rocks. Metamorphic chlorites vary widely in composition. Upper stabilities will vary depending on the composition, among other things. Generally, chlorites will persist up to temperatures between 450°C to 500°.

Expanding Clay Minerals

Expanding clay minerals, as discussed herein include fully expanding clays such as montmorillonite and vermiculite, as well as partially expanding mixed-layer clays such as illite/smectites, chlorites/vermiculites, etc. Expanding clays can be highly aluminous in composition (dioctahedral) or poor in aluminum and rich in Mg and/or Fe (trioctahedral). It is important to distinguish between the dioctahedral and trioctahedral varieties because their thermal stabilities are quite different.

Table 5 is a condensed version of a summary prepared by Velde (1977) which shows reported thermal stabilities of fully expandable clays and mixed-layer phases. It is important to note that the values given in Table 6 may be somewhat higher than the true thermal stability values of these clays. This situation arises because it is difficult to establish if equilibrium has been attained in hydrothermal synthesis studies of systems such as these. Reaction rates are so slow in these systems that it may be impossible to attain equilibrium over a period of weeks or months (times used for most of the runs that have been reported). Fully expanded and mixed-layer dioctahedral clays are stable to much higher temperatures if octahedral Mg is present or if Na or Ca (rather than K) predominates as the interlayer cation.

Although it is possible that Ca and/or Na in the interlayer will effect a much higher upper stability limit for dioctahedral smectites, it is also plausible that the run products observed in hydrothermal synthesis studies were not at equilibrium. Roberson and Lahann (1978) have shown that both Na and Ca greatly reduce the reaction rate of smectite/illite.

The most spectacularly high values representing upper stability limits for smectites are those for the trioctahedral smectites (hectonite and trioctahedral beidellite). Iiyama and Roy (1963) report that these trioctahedral smectites are stable up to 800°C at 1-2 kb pressure. Eberl, Whitney, and Khouri (1978) recently showed that K-saponite is still fully expanded after heating between 300°-485°C for 34 days at 2 kb. Although there may be some question as to whether equilibrium was obtained in these studies, it is clear that trioctahedral smectites can be expected to persist to great depths. Wilson, et al. (1968) reported that trioctahedral smectites have been observed in metamorphosed carbonate rocks in Scotland.

Studies of Gulf Coast Tertiary sediments by Perry and Hower (1970) show that mixed-layer illite/smectite persists to depths of over 16,000 ft and temperatures of up to nearly 200°C. The percentage of smectite in these mixed-layer clays decreases monotonically with depth. The character of the mixed layering also changes with depth. Random mixed layering gives way to an allevardite-like ordered mixed-layer phase at about 100°C. Studies by Velde (1969) of the muscovite-pyrophyllite system, allow us to compare stability ranges of mixed-layer illite/smectite phases in a controlled, simplified, synthetic system with those of a comparable natural system. Figure 22 from Velde (1977) shows the phases in the muscovite-pyrophyllite join. Although the sequence of change is very similar to that observed in the natural system, the temperatures observed by Velde are considerably higher than temperatures observed in the natural system. For example, the upper stability of mixed-layer illite/smectite in the Gulf Coast is shown to be about 200°C, Velde's studies would indicate an upper stability of about 400°C. The higher temperatures observed by Velde suggest that equilibrium was not obtained. Alternatively, the simplified chemical system studied by Velde may be sufficiently different from the natural system to cause major differences in thermal stabilities. Velde (1977) prepared a depth-temperature plot of natural mineral assemblages for fully expanding phases, random and ordered mixed-layer phases, and an ordered allevardite-type phase. The data for Velde's plot were obtained by several different investigations in studies of sediments of Tertiary age and younger.

It is clear from the data available to date that mixed-layer illite/smectite, with an ordered allevardite-type stacking (with approximately 30% smectite layers) can be expected to persist to at least 200°C. Whether or not this phase can be expected to occur at greater temperatures and pressures cannot be answered at the present time.

Trioctahedral smectites and/or mixed-layer trioctahedral smectite/chlorite are reported in rocks that have undergone heating at depth. Closer examination of fine grained Mg-rich metamorphic rocks may show that this occurrence is not at all unique.

MECHANICAL PROPERTIES OF CLAYS UNDER HIGH PRESSURES

Knowing that gouges have a high proportion of clays and such clays can exist at depths of up to perhaps 12 km, it is logical to find out the properties of component clays under high pressures. Although the behavior of clays under differential stresses are of great importance in soil mechanics, most of the tests are performed under a few bars of confining pressures under drained or undrained conditions. Recently experiments were performed by Summers and Byerlee (1976) and Shimamoto (1977) with clays sandwiched in between surfaces in triaxial experiments. They found a drastic lowering of frictional strength with montmorillonite and vermiculite gouge in particular. In Summers and Byerlee's (1976) and Shimamoto's (1977) experiments with many types of simulated gouge, the strength was determined by the gouge-rock contact. For the clay gouge in Summers and Byerlee's experiments, it is possible that the clay water is actually under partially drained condition, as the water in the clay can escape into the surrounding rock.

Since gouge is often massive enough such that the properties of whole clay are important in determining the behavior of the fault. For this reason we are performing experiments on cylindrical samples of clays without rock plugs under undrained conditions. The samples are prepared from clay powder by placing pouches of clays under confining pressure of 2-4 kb for 24 hours or more. The compressed clay is hard enough that it can be machined with ease. Similar to experiments in soil mechanics, the clay samples so prepared can undergo large strain but are still able to bear stress; quite often an experiment is terminated because the available travel of the piston is used up, rather than because the sample has lost strength completely. Details of the experiment are described in papers by Wang et al. (1979a, 1979b).

Figure 8 shows three examples of stress-strain curves for montmorillonite. In the figures, ε_z represents axial strain as sensed by foil strain gages attached to the cylindrical wall of the sample, ε_u is that computed from external displacement gages. Notice the close agreement of these two values when ε_z is less than about 15 percent; when ε_z exceeds 15 percent, the gage may be affected by excessive deformation underneath it. ε_θ denotes the lateral strain and ε_v the calculated volume strain $\frac{\Delta V}{V}$.

Figures 8 show clear peak strengths and with further strain, residual strength. The curves resemble those for overconsolidated clay in soil mechanics. As consolidation refers to the decrease of pore fluid under confining pressure the material is undersaturated or that the effective stress is higher than a saturated clay under the same condition. The explanation offered in soil mechanics for such phenomenon is that after peak strength is reached the grains in a certain region gradually rotate to follow the same general direction, and the residual strength is the frictional strength of sliding along this zone. Under normal consolidation, i.e., in saturation, the barrier for grain rotation is essentially removed. The residual strength for the two states are found in soil mechanics to be indistinguishable. Both the residual or "ultimate" strength and the peak strength are likely to be of interest in the fault zone if the gouge controls the fault behavior, as the gouge has undergone extensive straining beforehand, however, the slipping surfaces do not have uniform orientation.

The montmorillonite results are quite remarkable in that the peak strength varies only slightly with confining pressure especially for σ_r > 3 kb as summarized in Figure 9. This phenomenon may be related to the closing or pore space, and the rise in pore pressure of the water, therefore the near constancy of effective stress. The maximum shear strengths in this case are only 0.25 to 0.35 kb and are much smaller than those needed to activate a stick-slip with rock-on-rock contact (Byerlee, 1978), or stick-slip experiments with thin clay gouge layers (Summers and Byerlee, 1976). The residual shear strength is even smaller. Wang et al. (1979b) have also shown that illite, kaolinite and chlorite are somewhat stronger, of the order 0.6-0.9 kb.

Further tests are anticipated to investigate the influence of pore pressure, mineralogy, and temperature.

DISCUSSION

The formation of fault zones could involve several processes. In this section, we shall provide a conceptual sequence of the events in a fault zone based on field observations, rock mechanics, and intuition. Only the shallow part, i.e., above 12 to 15 km, of the zone concerns us here, assuming that flow rather than sudden slips is taking place below the level of 12 to 15 km (Sibson, 1977).

Major fault zones probably form by joining lesser weaknesses. As a result, the fault is likely to be irregular in shape to start with. The smaller irregularities or asperities will be broken off first, as the stress concentration there will be high; the broken rock will be caught up in the fault zone, and be further reduced in size as displacement along the fault continues. The amount of the intrafault materials should thus be related to the volume of asperities broken off. There may also be several parallel or subparallel weaknesses in the area, these may have movements on them initially, until a dominant fault forms, then the activities on these subsidiary faults would decrease.

Although the larger asperities may last for a time, repeated loading and rapid unloading and the stress concentrations on them may cause the formation of new joints. Jointed blocks near the fault zone could easily be "plucked" from the wall to go into the fault zone. The jointed rocks in the vicinity of the fault and the fault zone itself would form an excellent water conduit as well as reservoir.

The finely ground rocks have increased free energy and will soon be able to transform to new minerals that are consistent with the local T, P conditions, pH of pore fluid and overall chemistry. These are most probably clay minerals of various kinds. The large blocks caught up in the fault zone may also be altered to some extent.

The fault zone resulted from the processes described above is a complex system with subsidiary faults and densely jointed rocks nearly, a heterogeneous mixture of fault zone materials and the zone varies in width from place to place. Water may move around the fault zone under the influence of the stress-induced pressure gradients and continuous reaction of water with the fault breccia will further alter the mineralogy of the fault zone.

Based on available triaxial clay test data described in this report, we expect that a fault zone rich in expandable clays would have a shear strength of about 200 bars. With other clays, the strength will be in the range of 600-1000 bars. We should hasten to add here that temperature is one of the most important factors in the mechanical properties of clays. If higher temperature will weaken the clays or even lead to dehydration, then the numbers mentioned will be lowered correspondingly. The problem then involves the mechanisms for raising temperature and the rehydration of clays.

Curvature could evidently cause strength variation in the fault zone as well. If we have two asperities approaching each other (Figure 10), then the fault zone materials or even the asperities may have to be sheared through new planes before the fault can move with enough displacement to relieve the accumulated strain. It is often wondered whether the strongest point or the weakest will be the starting point, the hypocenter, of a large earthquake. Obviously, the strongest point has to yield before sufficient displacement can be achieved. On the other hand, if the motion at the weaker points will cause the strongest point to yield, a large earthquake can also result from it.

With the strength differences at different points in the fault zone, the strain field will not be uniform after a major displacement event. Such non-uniformity and the time-dependent behavior of the materials will then create aftershocks.

CONCLUSION

Clay gouge has been found in fault zones of very different ages and at different depths down to a depth of 2 km. Based on available clay stability studies, we can expect the gouge clays to be able to exist up to temperatures around 400°C for several dioctahedral clays and to 800°C for expandable trioctahedral clays; these temperatures correspond to depths to 15km or deeper.

Clays are quite weak mechanically, if they do exist extensively in mature fault zones, then we would expect low (~ hundreds of bars) shear stresses in faulting. For montmorillonite, the shear strength is as low as 200 bars. With higher temperatures, the strengths of clays can be lowered considerably.

ACKNOWLEDGEMENT

The support of USDI contract, 14-08-0001-16802 and 08-0001-G474 for this research is acknowledged.

Robert Albert did mucy of the mapping and sampling in Idaho; S. Kasza did the petrographic work for the Adirondacks fault zone. Dr. Barry Raleigh provided the samples from the San Andreas drill hole. Robert Albert and Michael Muller did the X-ray work.

Sincere thanks are extended to Bill Kopp, Garth Crobsy, Herb Harper, Stan Huff, Don Long, Joe Mendive, Norman Redford, Dwight Juras, Joe Luckini, and many others who made it possible for us to visit the deep mines in the Coeur d'Alene district, Idaho and freely gave us information concerning the fault zones in the mines.

References

Anderson, J.L., and R.H. Osborne, Summary Report, in USGS-OES Summaries of Technical Repts., Vol. VII, 469, 1978.

Byerlee, J., Friction of Rocks, PAGEOPH, 116, 613-626, 1978.

Clark, M.M., A. Grantz, and M. Rubin, Holocene activity of the Coyote fault as recorded in sediments of Lake Cahuilla. The Borrego Mtn. Earthquake of April 9, 1968, USGS Prof. Paper, 787, 1972.

Dunoyer de Segonzac, Les minéraux argileux daus la diagénese passage an métamorphism, Mem. Ser. Carte Geol. Alsace Lorraine, 29, 320 p., 1969.

Eberl, D., G. Whitney, and H. Khoury, Hydrothermal reactivity of smectite, Am. Mineralogist, 63, 401-409, 1978.

Fisher, D.W., Y.W. Isachsen, and L.V. Rickard, New York State Geologic Map, N.Y.S. Mus. and Sci. Serv. Map and Chart Ser. No. 15., 1970.

Hayes, J.B., Polytypism of chlorite in sedimentary rocks. Clays and Clay Min., 18, 285-306, 1970.

Hobbs, S.W., A.B. Griggs, R.E. Wallace, and A.B. Campbell, Geology of the Coeur d'Aleue District, Shoshone County, Idaho, USGS, Prof. Paper, 478, 1965.

Iiyama, J.T., and R. Roy, Controlled synthesis of heteropolytypic (mixed-layered) clay minerals. Clays and Clay Min., 10, 4-22, 1963.

Keller, W.D., Hydrothermal kaolinitization (endellization) of volcanic glassy rock. Clays and Clay Min., 10, 333-343, 1963.

Keller, W.D., and R.F. Hanson, Hydrothermal alteration of a rhyolite flow breccia near San Luis Potose, Mexico, to refractory Kaolin., Clays and Clay Min., 16, 223-229, 1968.

Long, G., L. Brown, and S. Kaufman, a reflection seismic profiles across San Andreas near Parkfield, Calif., in preparation, 1979.

Lowell, J.D., and J.M. Guilbert, Lateral and vertical alteration-mineralization zoning in porphyry ore deposits, Econ. Geol., 65, 373-408, 1970.

Muffler, L.J.P., and D.E. White, Active metamorphism of upper cenozoic sediments in the Salton Sea geothermal field and the Salton trough, southeastern California, Bull. Geol. Soc. Amer., 80, 157-182, 1969.

Perry, E.A. and J. Hower, Burial diagenesis in Gulf Coast pelitic sediments. Clays and Clay Min., 18, 165-178, 1970.

Procter, R.J., C.M. Payne, and D.C. Kalin, Crossing the Sierra Madre fault zone in the Glendora tunnel, San Gabriel Mountains, California, Eng. Geology, 4, 5-63, 1970.

Roberson, H.E., R. Lahann, and R.C. Campbell, Montmorillonite/Illite transformation rates: effects of solution chemistry. Clay Min. Soc. Abs., 56, 1978.

Shimamoto, T., Effects of fault gouge on the frictional properties of rocks: an experimental study, Ph.D. dissertation, Texas A and M Univ., 1977.

Sibson, R.H., Fault rocks and fault mechanisms, J. Geol. Soc. London, 133,191-213, 1977.

Summer, R., and J. Byerlee, A note on the effect of fault gouge composition on the stability of frictional sliding, Int. J. Rock Mech. Min. Sci., 14, 155-160, 1977.

Thompson, F.I., San Jacinto tunnel, Eng. Geol. in S. Calif., Special Publ., Assoc. of Eng. Geologists, 1966.

Velde, B., The compositional join muscovite-pyrophillite at moderate pressure and temperature, Bull. Soc. Fr. Mineral. Crist., 92, 360-368, 1969.

Velde, B., Clays and clay minerals in natural and synthetic systems, Elsevier, N.Y., 1977.

Wallace, R.E., Structure of a portion of the San Andreas rift in southern Calif., Bull. Geol. Soc. Am., 60, 781-806, 1949.

Wang, C.Y., W. Lin, and F.T. Wu, Constitution of the San Andreas fault zone at depth, Geophy. Res. Letters, 5, 741-744, 1978.

Wang, C.Y., N.H. Mao, and F.T. Wu, The mechanical property of montmorillonite clay at high pressure and implications on fault behavior, Geophysical Research Letters, in press, 1979a.

Wang, C.Y., N.H. Mao, and F.T. Wu, Mechanical properties of clays at high pressure, submitted for publication, 1979b.

Weaver, C.E., and K.C. Beck, Clay-water diagenesis during burial: how mud becomes gneiss, Geol. Soc. Amer., Special Paper, 134, 1971.

Wu, F.T., Mineralogy and physical nature of clay gouge, PAGEOPH, 655-689, 1978.

Wu, F.T., L. Blatter, and H. Roberson, Clay gouges in the San Andreas fault system and their possible implications. PAGEOPH, 113, 87-96, 1975.

Wilson, M.J., D.C. Bain, and W.A. Mitchell, Saponite from the Dalradian metalimestones of north-east Scotland, Clay Minerals, 7, 343-349, 1968.

List of Tables

Wall Rocks and their Mineralogy		
Schroon River Fault	I-87 Fault	Fault Zone
Meta-anorthosite	Dolomite	Alteration Mineralogy
plagioclase (andesine-oligoclase) partly sericitized hornblende orthopyroxene (trace) apatite (trace) biotite		hornblende → chlorite biotite → chlorite garnet → chlorite plagioclase → sericite → calcite + qtz + chlorite →stilpnomelene
Charnockitic Granitic Gneiss	Metagranite	
quartz plagioclase (andesine) 70-80% microcline-perthite hornblende opaques apatite biotite zircon chlorite sericite calcite	quartz plagioclase (oligoclase) 60-70% microcline hornblende biotite garnet chlorite zircon apatite	

Table 2

Percentages of Clay Minerals in Deep Mines In Idaho

	% Chlorite	% Illite	% Montmorillonite
Osburn Fault (21 Samples; 13 Gouges & 8 Rocks)			
Gouge	10.46 ± 10.86	84.08 ± 8.17	5.46 ± 4.58
Rock	6.25 ± 8.17	93.75 ± 8.17	0
Polaris Fault (23 Samples; 10 Gouges & 13 Rocks)			
Gouge	14.0 ± 7.13	86 ± 7.13	0
Rock	8.42 ± 3.23	91.57 ± 3.23	0
Cate Fault (15 Samples; 10 Gouges & 5 Rocks)			
Gouge	23.90 ±	70.9 ± 8.25	4.30 ± 2.50
Rock	11.60 ± 5.03	84.4 ± 8.29	2±0
Silver Syndicate Fault (13 Samples; 7 Gouges & 6 Rocks)			
Gouge	20.71 ± 8.14	73.29 ± 9.8	4.5 ± 4.35
Rock	15.67 ± 10.25	84.33 ±10.25	0
Morning - Independence Fault (16 Samples; 14 Gouges & 2 Rocks)			
Gouge	32.07 ± 19.70	48.85 ±21.90	18.78 ± 15

Table 3

Sample	% Kaolinite and/or Chlorite	% Illite	% Montmorillonite & Mixed Layer
TP 1	22	0	78
TP 2	0	0	100
TP 3	0	0	100
TP 4	19	0	81
TP 5	22	22	56
TP 6	0	0	100
TP 7	0	0	100
TP 8	0	0	100

Sample Depth (Ft.)	% Chlorite	% Kaolinite	% Illite	% Montmor.	% Mixed Layer	Density gm/cc
125	5	4	31	22	38	2.29
275	8	4	39	25	24	2.53
365	19	22	22	23	4	2.40
425	18	23	11	19	29	2.16
530	23	18	31	28	0	2.38
575	19	21	15	19	26	2.41
620	20	26	29	23	2	2.46
650	18	30	27	20	5	2.41
740	12	23	15	19	31	2.39
800	15	31	20	32	2	2.48
875	19	20	11	21	29	2.51
905	27	26	18	15	14	2.49

TABLE 4

Densities and clay compositions of the less than 2 microns fractions of gouge samples.

Table 5

Thermal Stabilities of Fully Expandable Phases

Type	Elements in 2:1 lattice	Reference	1-2Kb Pressure temp, °C
K dioct	(AlSI)	Velde, 1969	230
K dioct	(MgAlSi)	Velde, 1973	400
Na dioct	(AlSi)	Sand, et al., 1957 Koizumi and Roy, 1958	350-450
Ca dioct	(AlSi)	Chatterjee, 1959 Hemley, et al., 1971	300-500
Mg trioct	(MgSi)	Esquevin, 1960 Velde, 1973	<250
Mg trioct	(MgAlSi)	Velde, 1973	430
Na tricoct beidellite	(MgAlSi)	Iiyama and Roy, 1963	550
Na tricoct hectorite	(MgAlSiNa)	Iiyama and Roy, 1963	800

Thermal Stabilities of Mixed Layered Phases

K dioct	(AlSi)	Velde, 1969	400
K dioct	(AlSiMg)	Velde, 1972	430
Na trioct beidellite	(MgAlSi)	Iiyama and Roy, 1963	780
Na tricoct hectorite	(MgAlSiNa)	Iiyama and Roy, 1963	800

Figure Captions

Figure 1. Faults in southeastern Adirondacks, locations and geology.

Figure 2. Breccia surrounded by gouge in the Schroon River fault zone (from Farrar, 1976).

Figure 3. a -- unfaulted and unaltered gneiss (Schroon River Fault) (crossed nicols).
b -- Ferromagnesium minerals altered, almost completely, to chlorite. Chlorite forms streaks, parallel to the horizontal axis of the picture; the horizontal direction also is the preferred direction of the long axes of mineral grains (crossed nicols).
c -- Chlorite is the predominant mineral in this "gouge." Appears as dark green fine-grained rock. Some quartz and plagioclase appear as well rounded or subangular grains.

Figure 4. Angular dolomite breccia (edge marked by x) embedded in a fine grained matrix of dolomite, quartz and plagioclase.

Figure 5. Major faults in the Coeur d'Aleue district of northern Idaho (Hobbs et al, 1965).

Figure 6. Internal structures of Polaris fault at three depth levels in the Galena mine of Coeur d'Aleue district in northern Idaho.

Figure 7. Maps of different sections of the San Andreas fault zone; the locations of the sections are shown in the index map.

Figure 8. Stress and strain diagram for montmorillonite at 2kb σ_r is the confining pressure, σ_z the axial stress, ε_z, the axial strain. u, the percentage axial strain calculated from an external displacement transducer, ε_θ the lateral strain and ε_v the volume strain.

Figure 9. The peak strengths of montmorillonite clay as a function of confining pressures. The samples were pre-compressed, undrained, at 2kb.

Figure 10. When two "asperities" on a curved fault move into each other, new breaks through the fault zone will have to be made and wall rocks will have to be sheared off for further displacement.

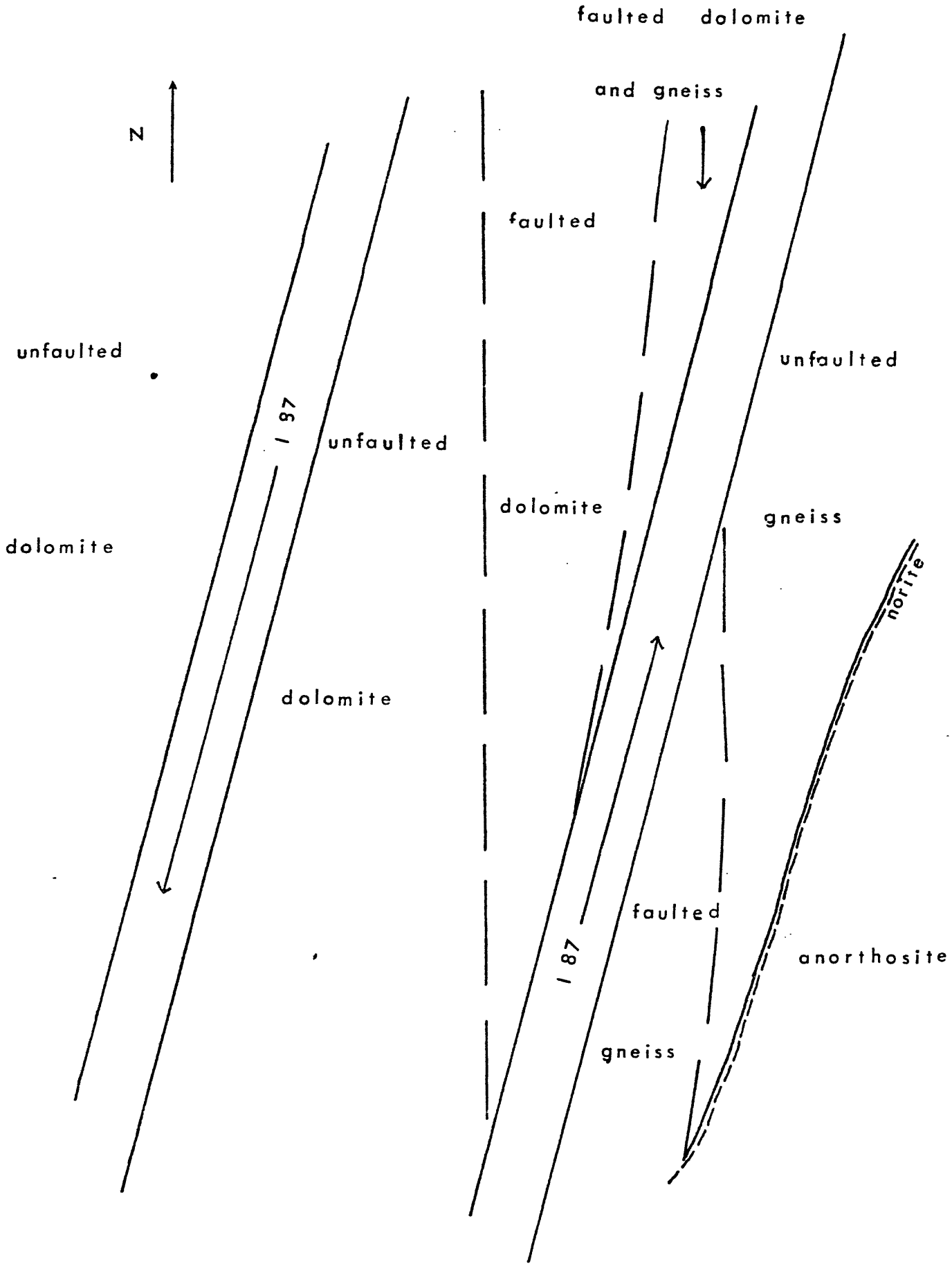
faulted dolomite
and gneiss
N
faulted
unfaulted
unfaulted
187
unfaulted
dolomite
gneiss
dolomite
norite
dolomite
faulted
187
anorthosite
gneiss

FIG 1a

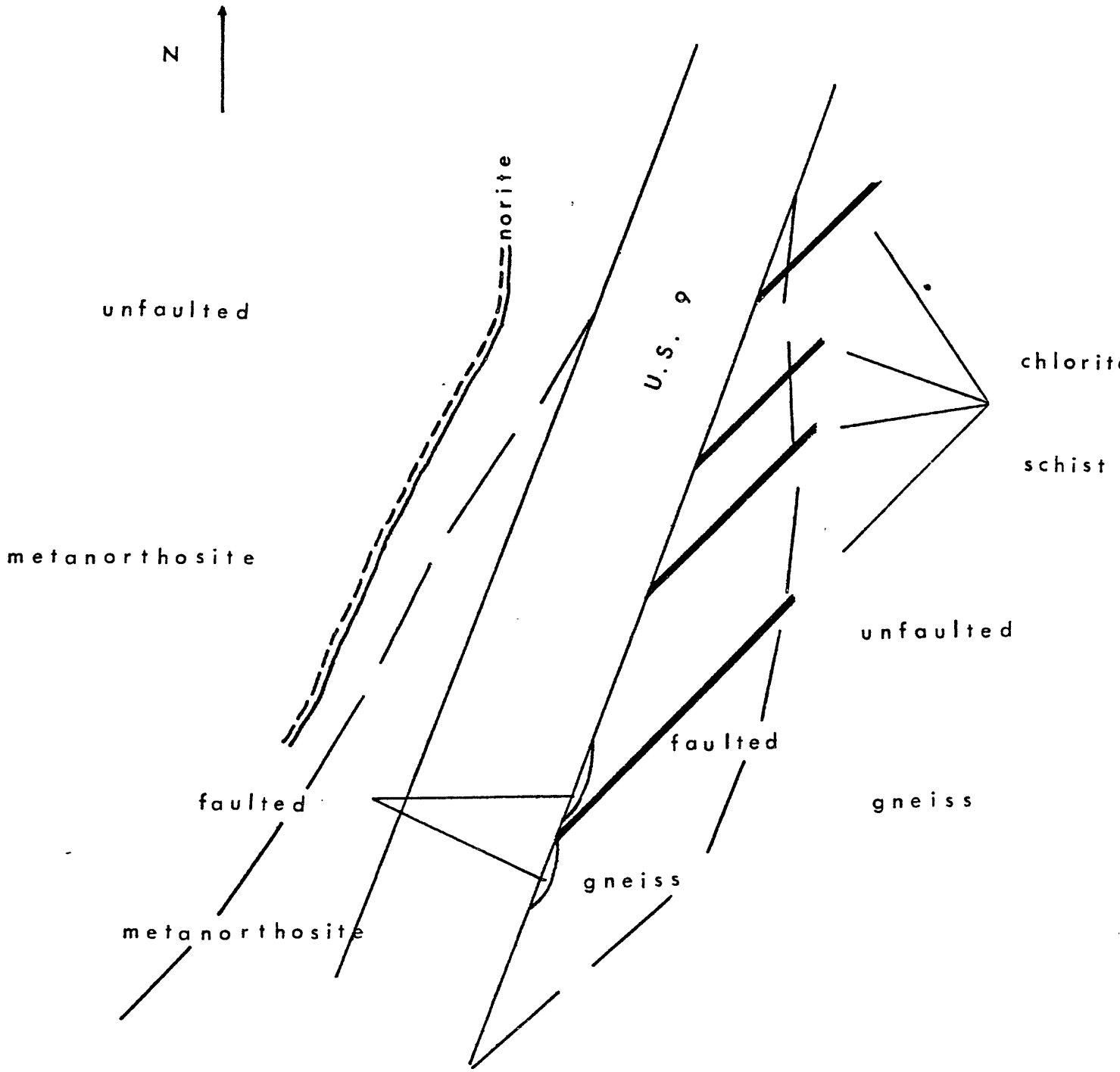
N
norite
unfaulted
U.S. 9
chlorite
schist
metanorthosite
unfaulted
faulted
faulted
gneiss
gneiss
metanorthosite

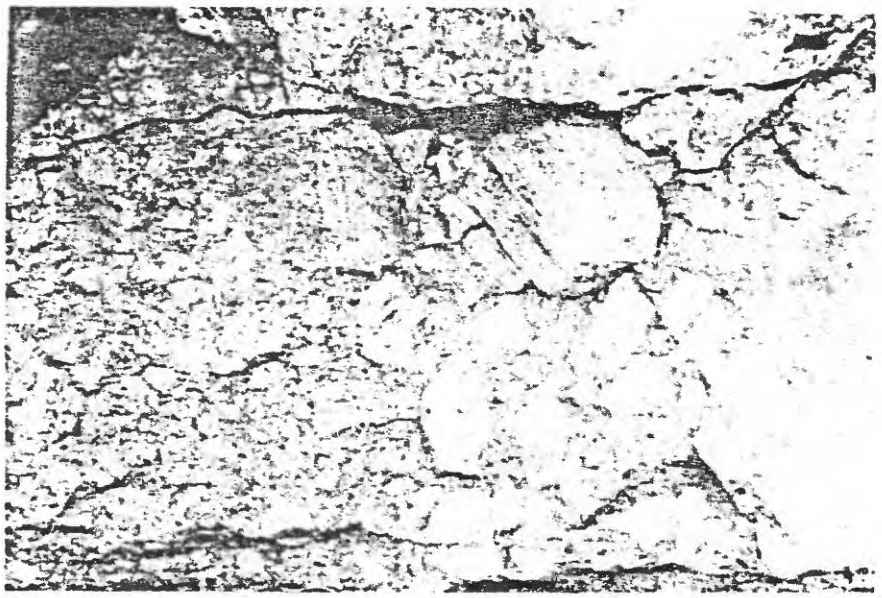

igure 65. Chlorite-calcite cemented breccia of charnc

FIGURE 2

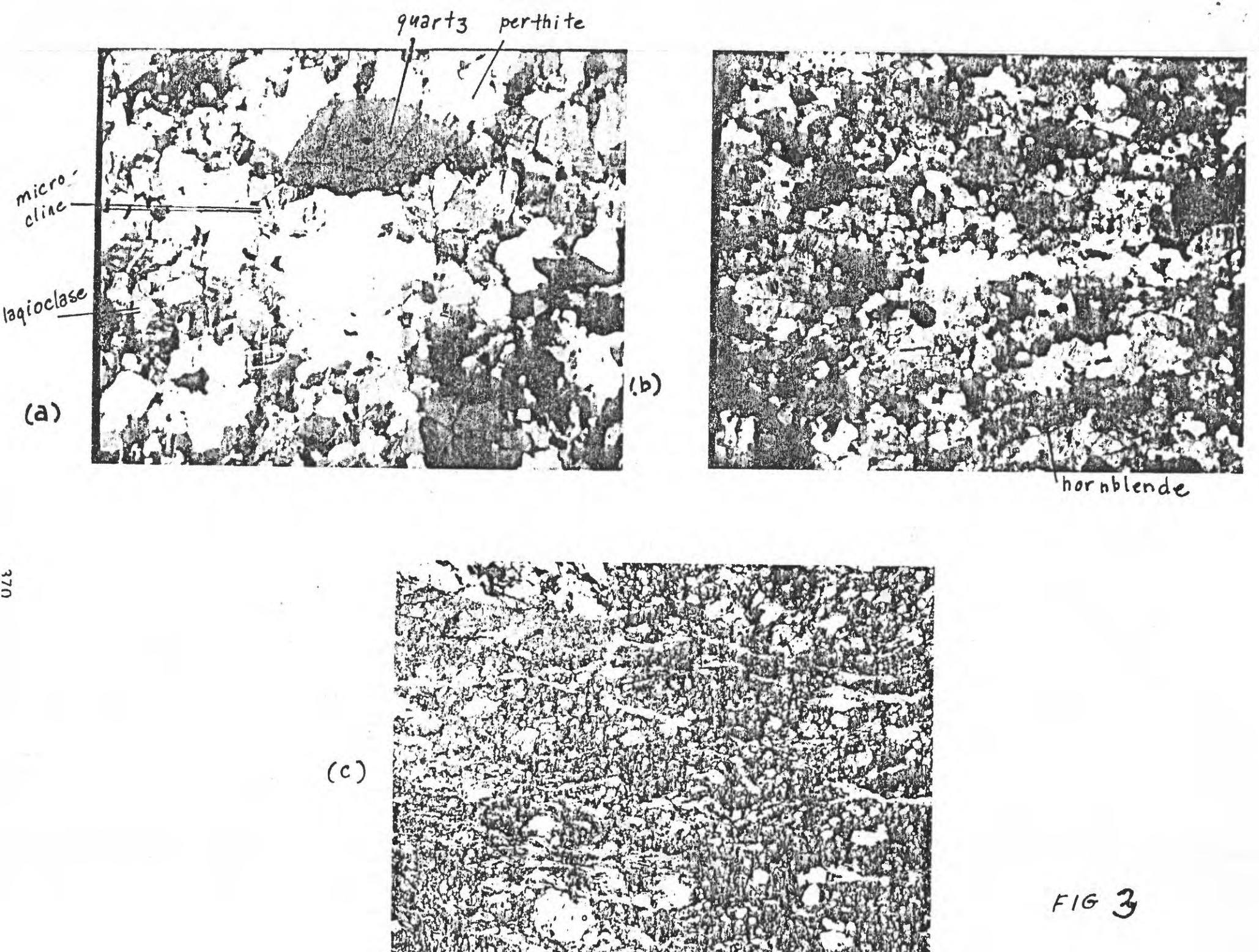

FIG 3

+ = edge of dol. clast

93, feldspar

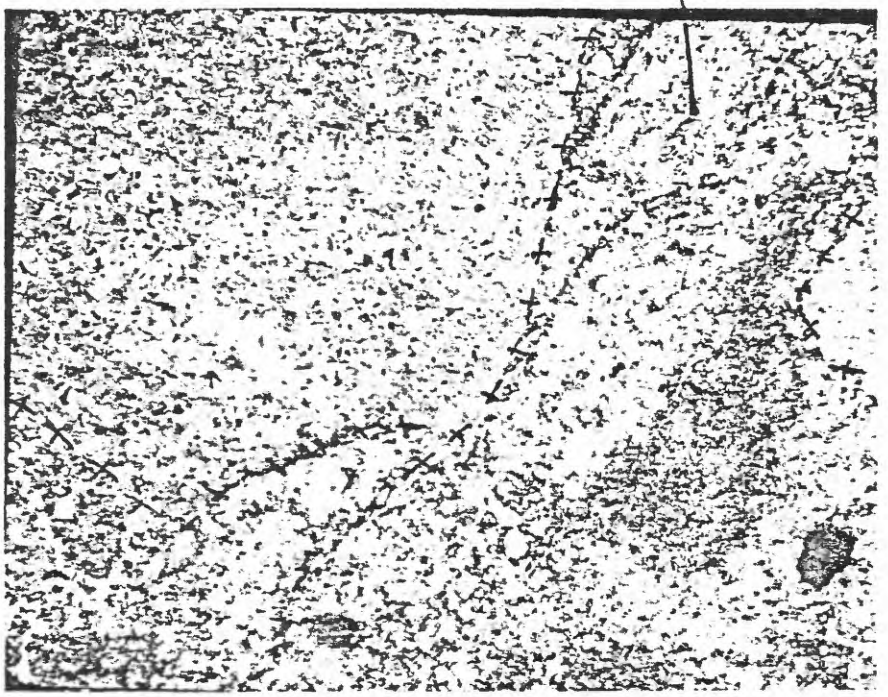

FIG 4

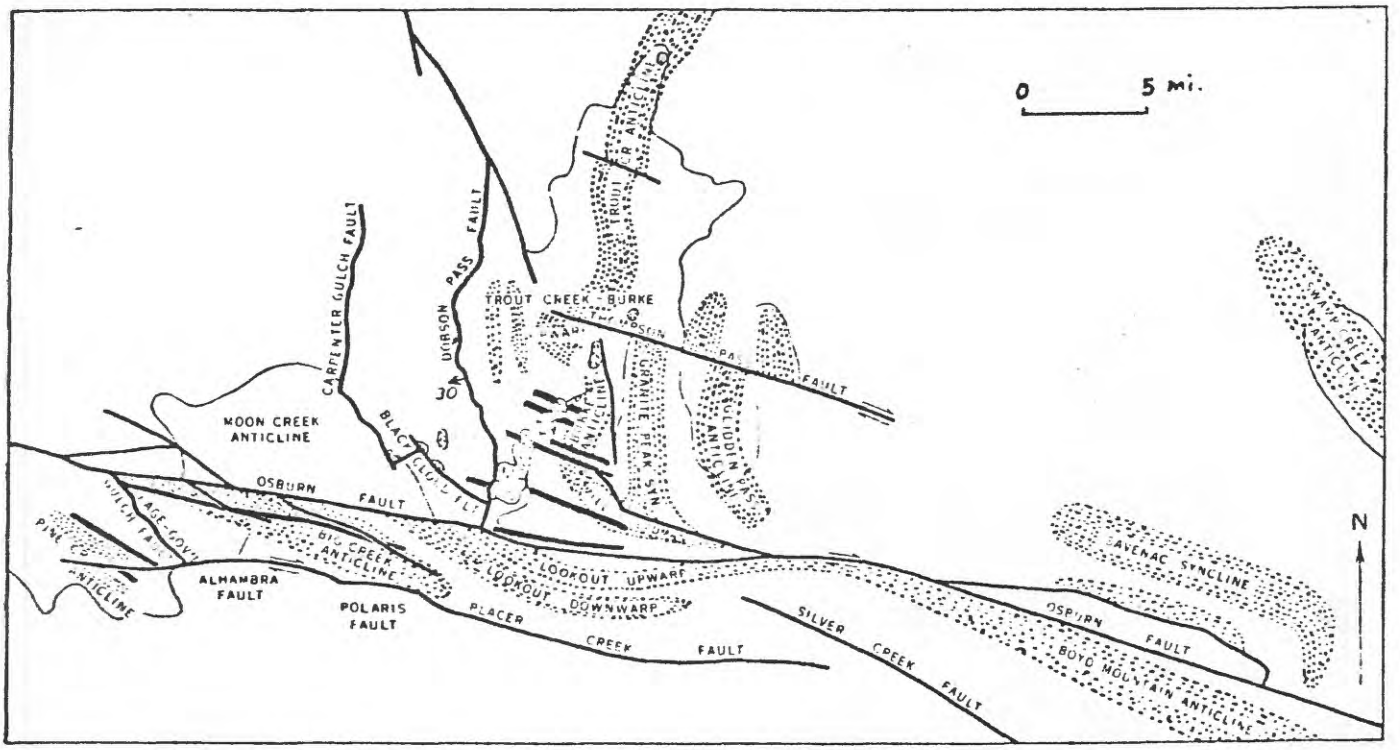

FIG 5

Galena Mine-Polaris Fault

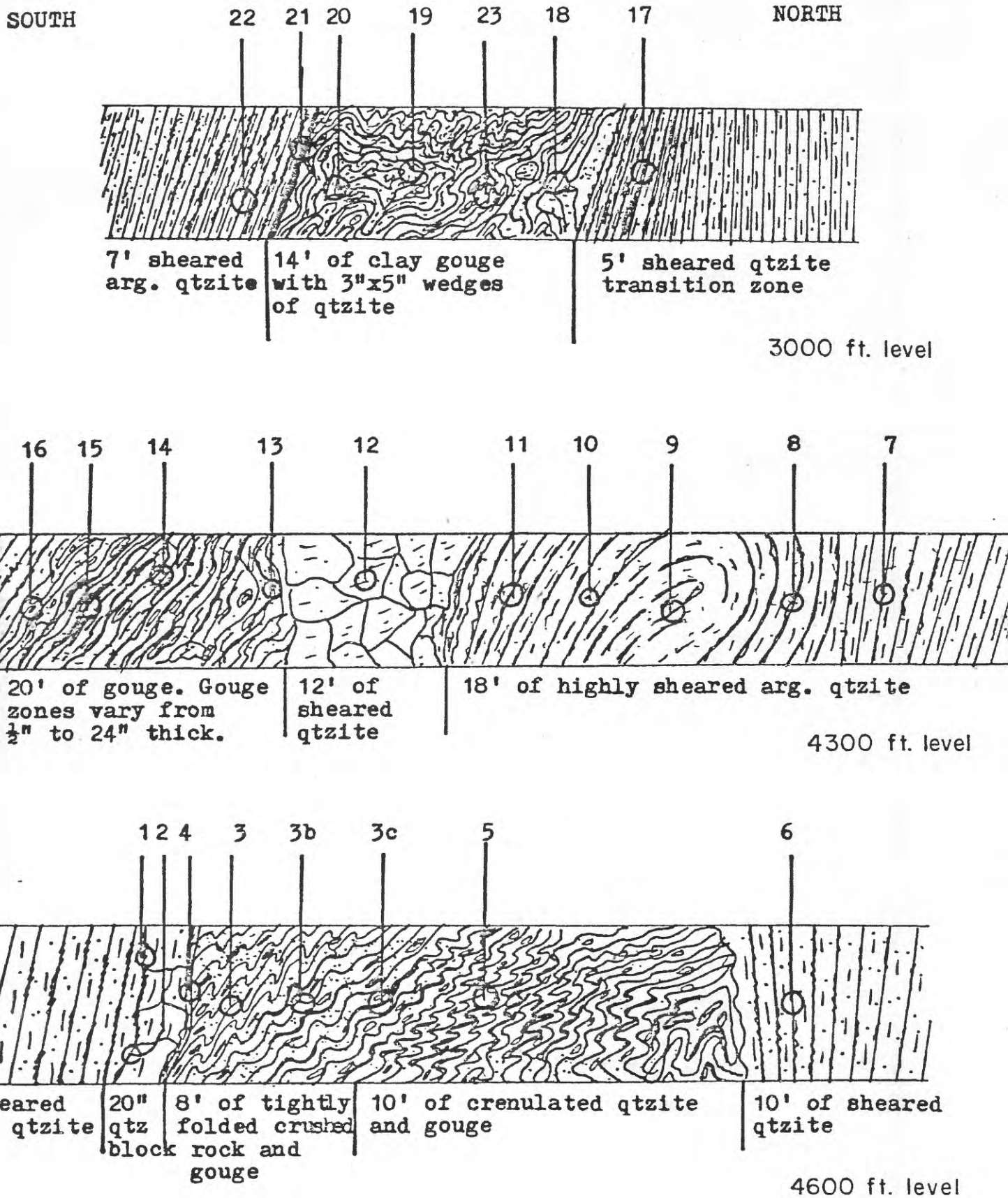

Figure 6

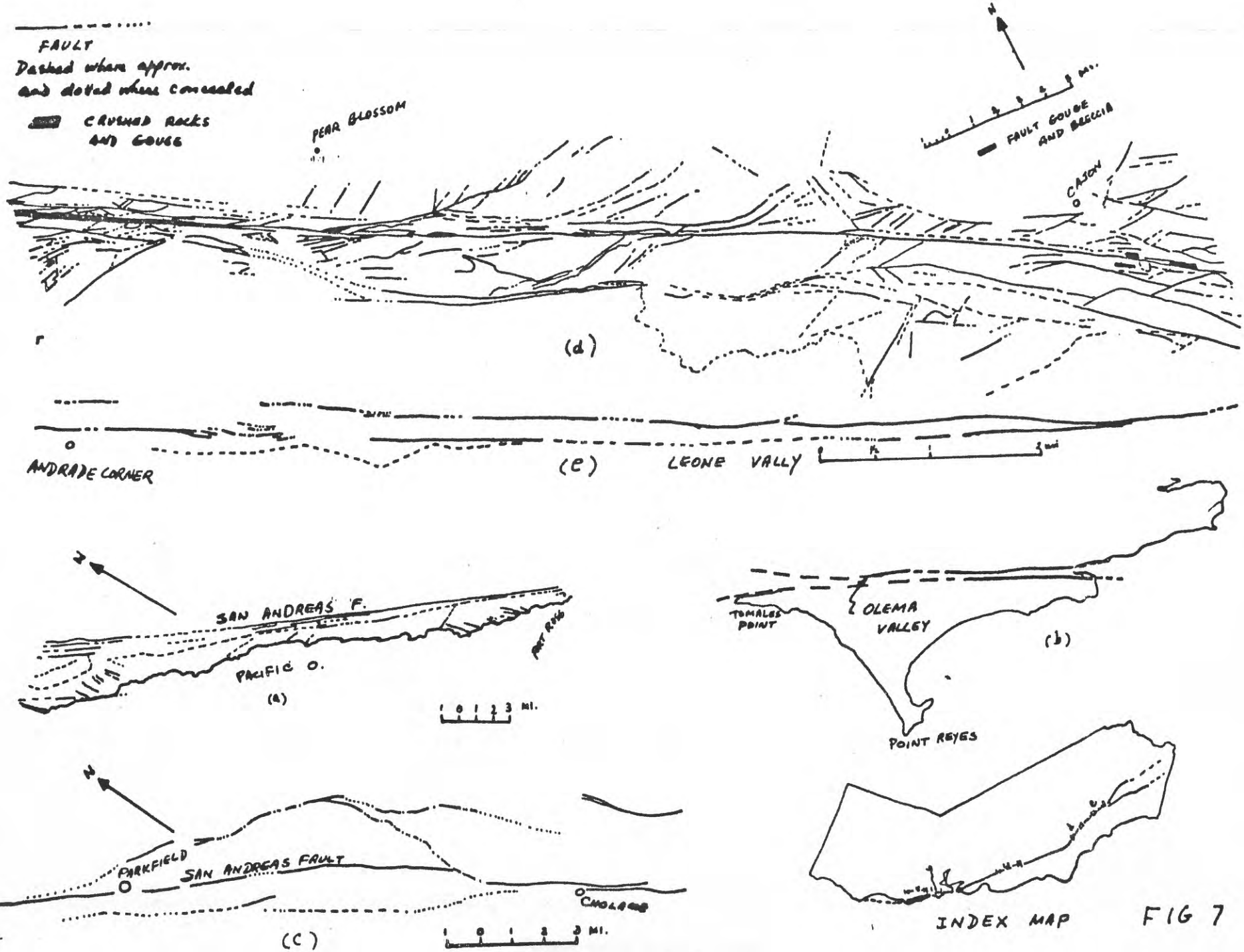
FAULT
Dashed where approx.
and dotted where concealed
CRUSHED ROCKS
AND GOUGE
FAULT GOUGE
AND BRECCIA
PEAR BLOSSOM
CAJON
(d)
ANDRADE CORNER
(e)
LEONE VALLY
SAN ANDREAS F.
PACIFIC O.
(a)
TOMALES
POINT
OLEMA
VALLEY
(b)
POINT REYES
PARKFIELD
SAN ANDREAS FAULT
CHOLAME
(c)
INDEX MAP

FIG 7

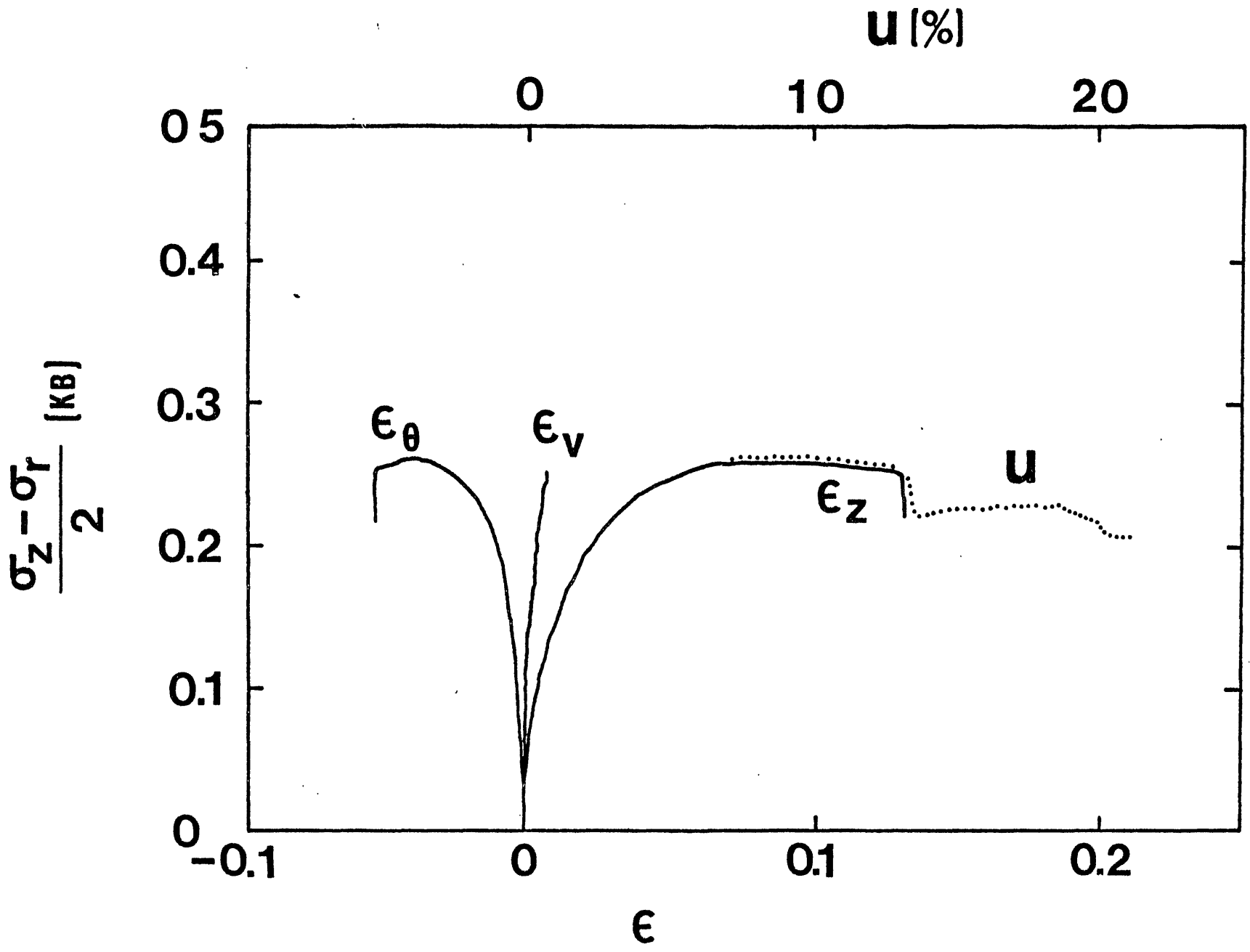
u [%]
0
10
20
0.5
0.4
0.3
0.2
0.1
0
$\frac{\sigma_z - \sigma_r}{2}$ [KB]
ϵ_θ
ϵ_v
ϵ_z
u
−0.1
0
0.1
0.2
ϵ

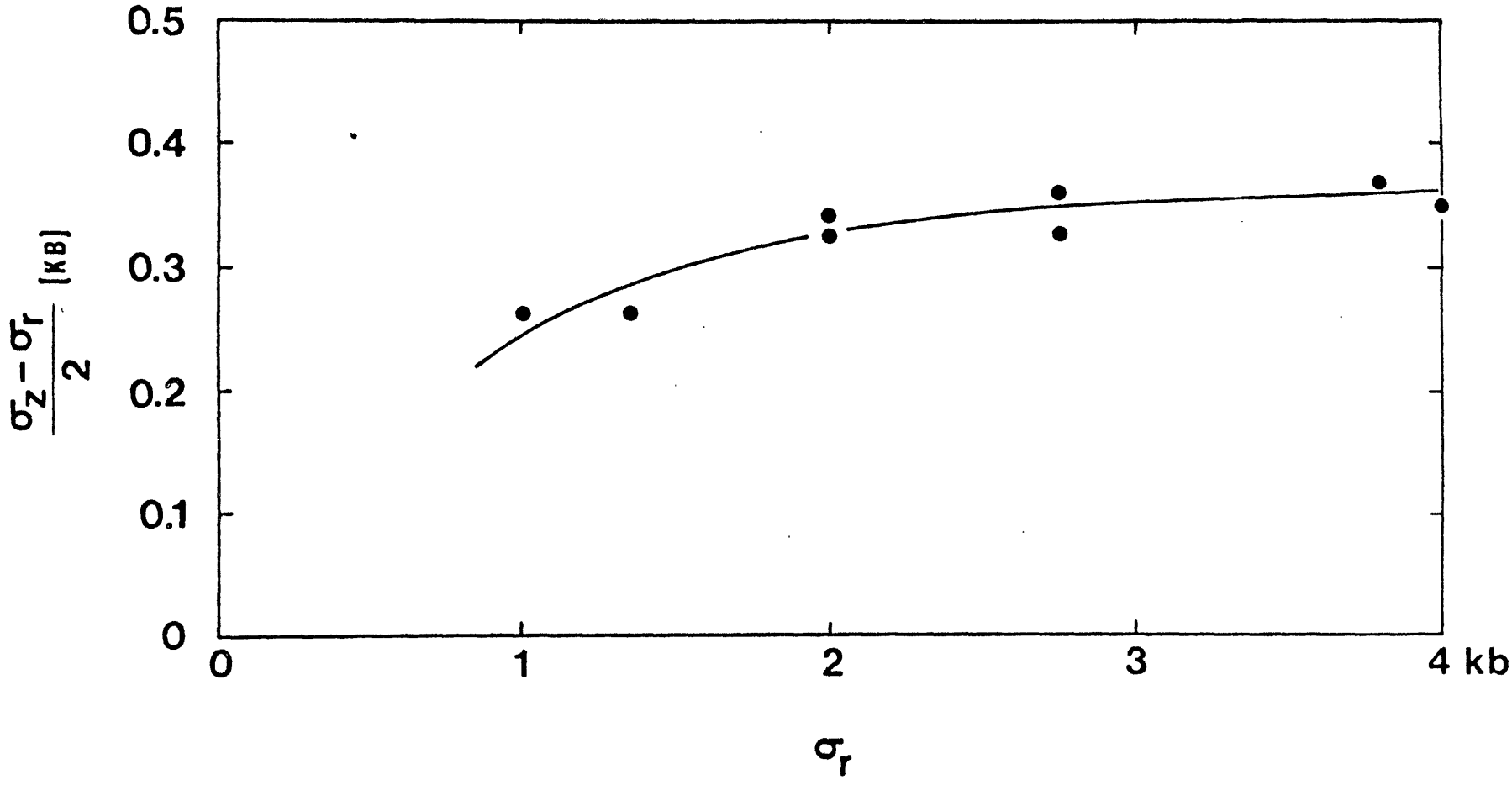

Fig. 9

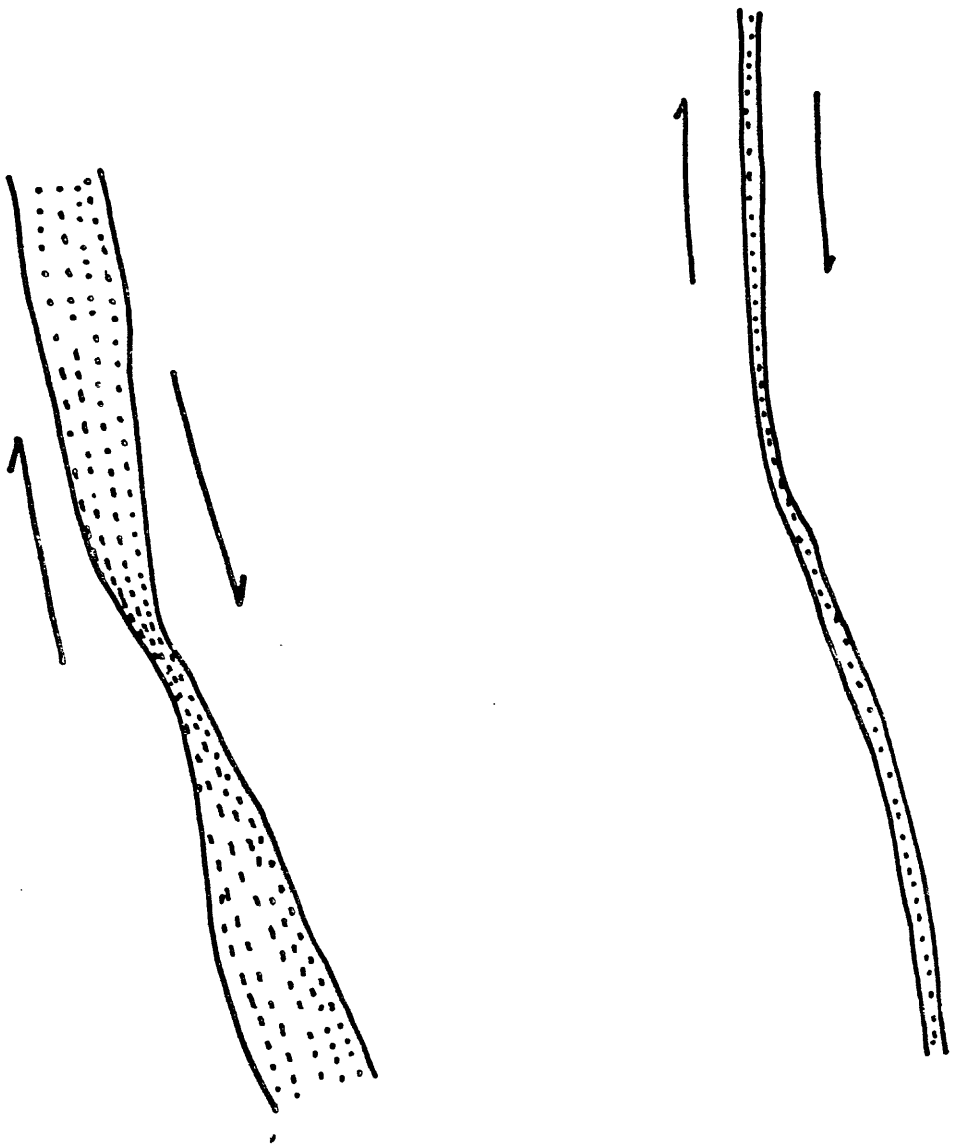

FIG 10

SEDIMENT SUBDUCTION

AND FRICTIONAL SLIDING IN THE SUBDUCTION ZONE

Chi-yuen Wang
Department of Geology and Geophysics
University of California, Berkeley 94720

Abstract

New experimental data for the mechanical and thermodynamic properties of clays at high pressure and high temperature are applied to model the frictional sliding in the subduction zone, based upon suggestions that much pelagic sediments have been subducted with the oceanic plate along active Pacific margins. This model is used to interpret the seismicity in the subduction zone and the heat flow across the arc-trench system.

Introduction

Sediments in the trenches along the Pacific margin are derived principally from turbidity currents that spread across the trench floor away from the island arcs and, in some cases, the continents. However, the ocean floor on the other side of the trench must also be a provider for the sediments in the trenches. Most of the Pacific ocean floor is covered with a layer of pelagic sediments which consist largely of various clays mixed with some organic ooze. The thickness of this layer varies from place to place; near the Pacific trenches, it is typically several hundred meters in thickness (Scholl et al., 1977). During the past 100-200 m.y., the active Pacific margins have been underthrusted by as much as 10^4 km of oceanic lithosphere.

The pelagic sediments are usually assumed to have been scraped off the subducted plate (e.g., Karig and Sharman, 1975). Scholl and Marlow (1974) argued, on the other hand, that several million cubic kilometers of pelagic material would appear in the fold belts rimming the Pacific, if the pelagic sediments were indeed scraped off the underthrusting plate. Geological studies of typical Pacific sedimentary sequences show, however, that only a few percent of pelagic-type deposit is present (Bailey et al., 1964; Blake et al., 1974; among others). Extensive seismic studies across the Peru-Chile trench (Hussong et al., 1976) suggested that almost all the sediments that entered the trench was subducted. Recent deep drilling in the Japan trench, the Mariana trench, and the Middle American trench (Geotimes, April 1978, October, 1978, and September, 1979, respectively) show that the amount of sediments in the trenches is far less than what one would expect if the sediments were scraped off the subducting lithosphere.

Counter evidences for the subduction of pelagic sediments are provided by Karig and Sharman (1975) using seismic reflection profiles in the trenches to show deformation and uplift of the pelagic sediments near the toe of the accretion prisms, and by Meijer (1974) using petrochemical data for the Mariana Island Arc volcanics to show that these volcanics are not contaminated by subducted sediments. On the other hand, more detailed seismic reflection profiles (Talwani et al., 1977) show that the deformation and uplift process is probably limited to the top section of the pelagic sediments; the lower sections are

subducted with the basement. Analyses of isotopic and trace elements in the Aleutian volcanics by Kay (1977) and others show that their special concentration in the volcanics could be explained by sediments and sea water contamination.

Thus the question is still open whether large portions of pelagic sediments at the trenches are subducted with the basement. On the other hand, the evidence for sediment subduction seems to be sufficiently strong for one to speculate about its consequences. In this communication, we utilize recent experimental data for the mechanical and thermodynamic properties of clays at high pressure and temperature, together with the pressure and temperature profiles along the upper surface of the subducted plate, to speculate on the effects of sediment subduction upon the frictional properties between the interacting plates.

Mechanical Property of Clayey Sediments

Summers and Byerlee (1977a) sandwiched thin layers of air-dried clays between rock pieces and studied the effect of clays on frictional sliding under high pressure. They found that the presence of montmorillonite and vermiculite in the rock joints greatly reduces the frictional resistance and stabilizes sliding between the rocks. The presence of illite, chlorite, and kaolinite, however, does not significantly lower the frictional resistance and violent stick-slips occur at high confining pressures. Summers and Byerlee concluded that presence of interlayer water in montmorillonite and vermiculite may

create a pseudo pore-pressure and stabilize sliding.

Upon saturation, pore-water influences the behavior of clays in two different ways: first, it affects mechanically the magnitude of stresses transmitted through the framework of mineral grains. Second, it affects the intrinsic property of clay particles by changing the state of hydration of the ions on the surface of each particle and thus modifying the contacts between them. Under low confining pressures, the available data in soil engineering literature show that the friction coefficient for saturated clays is much lower than that for dried clays (e.g. Lambe and Whitman, 1969). Wang and Mao (1979) recently studied the effect of saturated clays on sliding between rocks at high confining pressures. Part of their results is given in Figure 1 which shows that the shear stress required to initiate sliding is very much lower than that required for rock-on-rock sliding. For a given type of clay this shear stress increases linearly with the effective normal stress across the sliding surface. Joints filled with saturated montmorillonite show the lowest friction coefficient of 0.08; joints filled with saturated chlorite, kaolinite and illite show increasingly higher friction coefficients of 0.12, 0.15, and 0.22, respectively. Also shown in this figure is some results for sliding on rock joints filled with saturated fault gouge from the San Andreas fault zone, consisting primarily of a mixture of various clays and some clastics, mostly quartz. Preliminary analysis by Liechti and Zoback (1979) shows that the clays consist of about 47% montmorillonite, 34% of kaolinite, 10% of chlorite,

and 9% of illite. Experiments with these fault gouges show that the friction coefficient for the gouge-rock assemblage is 0.2-0.3. These coefficients may be compared with that for rocks (e.g. Byerlee, 1978), which is 0.8 at normal stresses less than 2 kb and 0.6 at normal stresses above 2 kb.

Also to be noted is that sliding is stable on all joints filled with saturated clays and fault gouges up to confining pressures of 3 kb, and appears to remain stable at least up to 6.3 kb for montmorillonite and vermiculite (Summers and Byerlee, 1977b).

A Model of Frictional Sliding in Subduction Zone

Assuming sediments are subducted, compaction of sediments will occur with increased burial and subduction. At the same time, water is being expelled. Permeability of the sediments decreases and the rate of escape of fluid is reduced. A portion of the water in the sediments may be trapped and retained to appreciable depth. Friction between the underthrusting and the overlying plates may be lowered if pore pressure in the sediments builds up. Even if pore pressure dissipates due to gradual loss of trapped water, friction would remain low if the sediments remain saturated. Furthermore, sliding will be stable and no seismicity is expected.

Under increasing overburden and rising temperature during continued subduction, the "free water" in the sediments is slowly driven away; thus the saturated sediments would gradually become dry. Comparing our experimental results with those of Summers and Byerlee

(1977a, b), we speculate that frictional resistance in the subduction zone will increase with depth as a result of loss of the trapped pore water. If the subducted sediments are composed largely of clastics or nonexpandable clays such as kaolinite, illite, and chlorite, continued shearing between the subducted and the overlying lithosphere would lead to violent stick-slips. On the other hand, if the subducted sediments are composed largely of expandable clays such as montmorillonite, sliding between the plates may remain stable even after the free water is largely lost.

Experimental studies of the stability fields of clays have been reviewed by Velde (1977); some results are given in Figure 2. Dehydration curves for kaolinite and chlorite have been constructed by Delany and Helgeson (1978), based upon low-pressure thermodynamic data. Two temperature profiles beneath the trench-arc system calculated by Minear and Toksöz (1970) and Andrews and Sleep (1974), respectively, are also given in Figure 2, partly to show the diversity in the results and partly to relate, in a qualitative way, the temperature profiles with the phase boundaries and the dehydration curves for clays. Precise comparison of these temperature profiles with the phase boundaries and dehydration curves for clays is meaningless, since the temperature calculations did not take into account the exchange of heat during dehydration or phase transition. The main point is that, in spite of the large uncertainty in the estimates of temperature in the subduction zone, the clays will undergo a phase transition and dehydration during their course of subduction. Raleigh and Peterson (1965), Heard and Rubey (1966), and Murrell and Ismail (1976) have demonstrated that

dehydration of various hydrous minerals under shear stresses causes embrittlement and failure of the host materials. Embrittlement and failure of the subducted sediments may also occur when the various clays dehydrate in the subduction zone, resulting in weak regions along the boundary between the interacting plates.

Figure 3 shows the salient features in the distribution of seismicity in the upper part of a typical subduction zone (modified from Molnar, 1979). At depths greater than 20-40 km in the underthrust zone, large seismic events with shear faulting mechanism occur between the overlying and the underthrusting plates. The fault plane involved could extend to much shallower depth. The question is why does the hypocenter appear at those depths? At very shallow depth beneath the trench, another zone of earthquakes occurs with mostly normal faulting mechanism. Between these two seismic zones the underthrust zone often has little seismic activity. Such pattern of seismicity is common for the Alask-Aleutian arc (Jacob et al., 1977), the Kurile-Kamchatka arc (Engdahl, 1977), the Japan arc (Engdahl et al., 1979), etc., and appears to be representative for most subduction zones around the Pacific Ocean. It is tempting to associate the aseismic region in the subduction zone with a region of low frictional resistance due to the presence of saturated clayey sediments. The seismic zone below about 40 km may correspond to a region where the subducted sediments have become dry under increasing pressure and temperature. Shear resistance in this zone is high, but may

still decrease as a result of dehydration of the clayey sediments, which leads to localized failure and subsequently earthquakes in the subduction zone. Formation of new minerals as a result of clay dehydration would cause further increases in the frictional resistance at the plate boundary. Eventually, the plate boundary may cease to be the weaker part of the subduction zone.

Heat Flow

A review of heat flow data across the trench-arc settings of the West Pacific was made by Watanabe and others (1977). In spite of large scatter, the values of heat flow are not randomly distributed; the average profile of heat flow, also shown in Figure 3, has the following common characteristics (Anderson et al., 1976): (1) the zone from the trench axis to the volcanic arc has abnormally low heat flow; and (2) the volcanic zone and the back-arc basins have high but variable heat flow. Such distinctive heat flow pattern seems to persist around the active Pacific margins.

In most calculations for the thermal state in arc-trench systems (e.g., Turcotte and Oxburgh, 1969; Minear and Toksöz, 1970) the above peculiar pattern of heat flow was not predicted. In order to keep the calculated heat flow between trenches and volcanic arcs as low as the observed values, Hasebe et al., (1970) found it necessary to assume that there is no frictional heating between the interacting plates at shallow depths but that frictional heating is "turned on" at depths greater than 60 km. Later, Anderson et al. (1976) noted that dehydration

of the ocean crust can effectively negate the friction heat. Deposition of sediments from the arc side may also lower the observed heat flow. Our model of frictional sliding in the subduction zone predicts low frictional heating in the aseismic zone and high frictional heating in the seismic zone along the interplate boundary and is thus consistent with the observed distribution of surface heat flow across the arc-trench system.

Summary

A model for the frictional sliding in the subduction zone is proposed, based upon the assumption that pelagic sediments have been subducted with the oceanic plate along active Pacific margins. The model is constructed using new experimental data for the mechanical and thermodynamic properties of clays at high pressure and high temperature and is shown to be consistent with the seismicity in the subduction zone and the heat flow across the trench-arc settings along the Pacific margin.

Acknowledgements

I benefit from discussions with Hal Helgeson, E.R. Engdahl, Tom Jordon, and Marcus Langseth. Francis Wu and George Brimhall read a previous version of this paper and provided helpful comments. Walter Alvarez and Larry Benson called my attention to some important references. This research is supported in part by a USGS grant USDI-14-08-0001-17747.

References

Anderson, R.N., S. Uyeda and A. Miyashiro (1976). Geophysical and geochemical constraints at convergent plate boundaries, I: Dehydration in the downgoing slab. Geophys. J. Roy. Astr. Soc. 44, 333.

Andrews, D.J. and N.H. Sleep (1974). Numerical modeling of tectonic flow behind island arcs. Geophys. J. Roy. Astr. Soc. 38, 237.

Bailey, E.H., W.P. Irwin and D.L. Jones (1964). Franciscan and related rocks, and their significance in the geology of western California. Calif. Div. Mines and Geol. Bull. 183, 177 p.

Blake, M.C. Jr., D.L. Jones and C.A. Landis (1974). Active continental margins, contras between California and New Zealand. In: Burk, C.A. and C.L. Drake (Eds.), The Geology of Continental Margins, 853. Springer-Verlag: New York.

Byerlee, J. (1978) Friction of rocks. Pageoph. 116, 615.

Delany, J.M. and H.C. Helgeson (1978). Calculation of the thermodynamic consequences of dehydration in subducting oceanic crust to 100 kb and 800°C. Am. J. Sci. 278, 638.

Engdahl, E.R. (1977). Seismicity and plate subduction in the central Aleutians. In: Talwani, M. and W.C. Pittman III (Eds.), Island Arcs, Deep Trenches and Back-Arc Basins, 259. Am. Geophys. Union: Washington, D.C.

Engdahl, E.R., N. Umino and A. Takagi (1979). Seismicity patterns related to the occurrence of interplate earthquakes off the coast of Northeastern Japan. EOS 60, 312 (Abstract).

Hasabe, K., N. Fujii and S. Uyeda (1970). Thermal processes under island arc. Tectonophys. 10, 335.

Heard, H.C. and W.W. Rubey (1966). Possible tectonic significance of transformation of gypsum to anhydrite plus water. Spec. Pap. Geol. Soc. Am. No. 76, 77.

Hussong, D.M., P.B. Edwards, S.H. Johnson, J.F. Campbell and G.H. Sutton (1976). Crustal structure of the Peru-Chile trench: 8°-12°S latitude. In: Sutton, G.H., M.H. Manghnani, R. Moberly and E.U. McAfee (Eds.), The Geophysics of the Pacific Ocean Basin and Its Margin, Am. Geophys. Union Mono. 19, Washington, D.C.

Jacob, K.H., K. Nakamura and J.N. Davies (1977). Trench-volcano gap along the Alaska-Aleutian arc: facts and speculations on the role of terrigenous sediments for subduction. In: Talwani, M. and W.C. Pittman III (Eds.), Island Arcs, Deep Trenches and Back-Arc Basins 243, Am. Geophys. Union: Washington, D.C.

Karig, D.E. and G.F. Sharman III (1975). Subduction and accretion in trenches. Geol. Soc. Amer. Bull. 86, 377.

Kay, R.W. (1977). Geochemical constraints on the origin of Aleutian magmas. In: Talwani, M. and W.C. Pittman III (Eds.), Island Arcs, Deep Trenches and Back-arc Basins, 229, Am. Geophys. Union: Washington, D.C.

Lambe, T.W. and R.V. Whitman (1969). Soil Mechanics. John Wiley and Sons: New York.

Liehti, R. and M.D. Zoback (1979). Preliminary analysis of clay gouge from a well in the San Andreas fault zone in central California (manuscript).

Meijer, A. (1974). A study of the geochemistry of the Mariana Island Arc system and its bearing on the genesis and evolution of volcanic arc magmas, Ph.D. Dissertation, Univ. of California, Santa Barbara, 214 pp.

Minear, J.W. and M.N. Toksöz (1970). Thermal regime of a downgoing slab and new global tectonics. J. Geophy. Res. 75, 1397.

Molnar, P. (1979). Earthquake recurrence intervals and plate tectonics, Bull. Seism. Soc. Am., 69, 115.

Murrell, S.A.F. and I.A.H. Ismail (1976). The effect of decomposition of hydrous minerals on the mechanical properties of rocks at high pressures and temperatures. Tectonophys. 31, 207.

Raleigh, C.B. and M.S. Paterson (1965). Experimental and deformation of serpentinite and its tectonic implications. J. Geophy. Res. 70, 3965.

Scholl, D.W. and M.S. Marlow (1974). Sedimentary sequences in modern Pacific trenches and the deformed circum-Pacific eugeosyncline. In: Dott, R.H. Jr. and R.H. Shaver (Eds.), Modern and Ancient Geosynclinal Sedimentations, 193. Soc. Econ. Paleontologists and Mineralogists Spec. Pub. 19.

Scholl, D.W., M.S. Marlow and A.K. Cooper (1977). Sediment subduction and offscrapping at Pacific margins. In: Talwani, M. and W.C. Pittman III (Eds.), Island Arcs, Deep Sea Trenches and Back-Arc Basins, 199, Am. Geophys. Union: Washington, D.C.

Summers, R. and J. Byerlee (1977a). A note on the effect of fault gouge composition on the stability of frictional sliding. Int. J. Rock. Mech. Min. Sci. & Geomech. Abstr. 14, 155.

Summers, R. and J. Byerlee (1977b). Summary of results of frictional sliding studies, at confining pressures up to 6.98 kb, in selected rock materials. USGS Open-file report 77-142.

Talwani, M., C.C. Windisch, P.L. Stoffa, P. Buhl, and R.E. Houtz (1977). Multichannel seismic study in the Venezuellan Basin and the Curacao Ridge. In: Talwani, M. and W.C. Pittman III (Eds.), Island Arcs, Deep Trenches and Back-arc Basins, 229, Am. Geophys. Union: Washington, D.C.

Turcotte, D.L. and E.R. Oxburgh (1969). A fluid theory for the deep structure of dip-slip fault zones. Phys. Earth Planet. Int. 1, 381.

Velde, B. (1977). Clays and Clay Minerals in Natural and Synthetic Systems, 318 pp. Elsevier: Amsterdam.

Wang, C.Y. and N.H. Mao (1979). Shearing of rock joints with saturated clays at high confining pressures. Geophys. Res. Lett. 6, 825.

Watanabe, T., M.G. Langseth and R.N. Anderson (1977). Heat flow in back-arc basins of the Western Pacific. In: Talwani, M. and W.C. Pittman III (Eds.), Island Arcs, Deep Sea Trenches and Back-Arc Basins. Am. Geophys. Union: Washington, D.C.

Figure Captions

Figure 1. Shear stress required to initiate sliding on rock joints filled with various saturated clays and fault gouge, plotted against the effective normal stress across the sliding surface. Also plotted is the relation for rock-on-rock sliding.

Figure 2. Phase boundaries and dehydration curves for various clays plotted on a depth-temperature space. Also shown are two temperature profiles calculated for the upper surface of the subducted plate. M stands for montmorillonite, A for allevardite, I for illite, and Ch for chlorite. The phase boundaries are taken from Velde (1977); the dehydration curves are from Delany and Helgeson (1978).

Figure 3. Schematic representation of the seismicity in the upper section of a subduction zone and the average heat flow profile across an arc-trench system (see text for more detailed description).

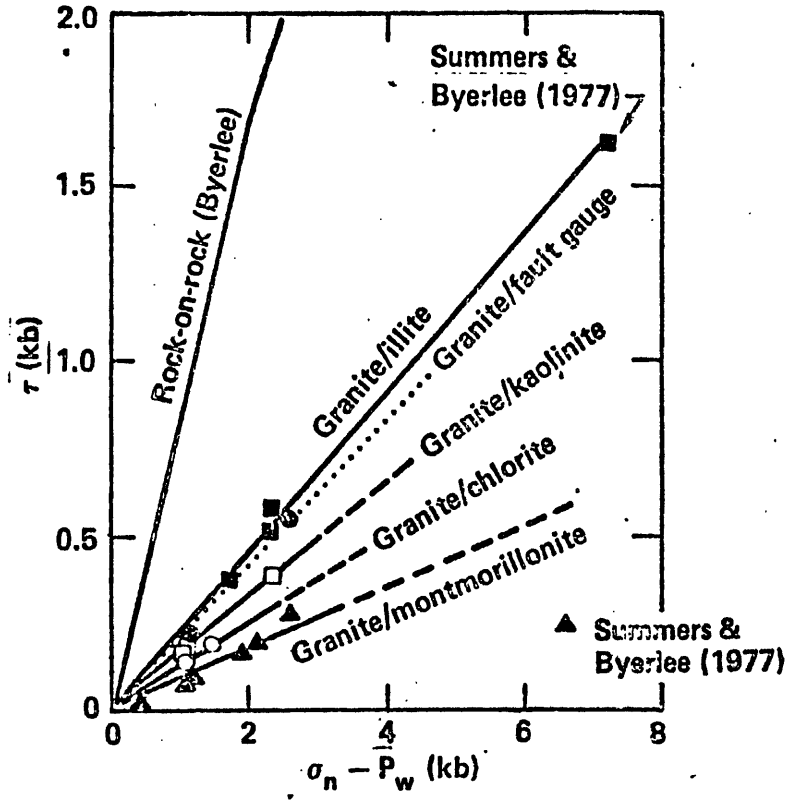

Figure 1

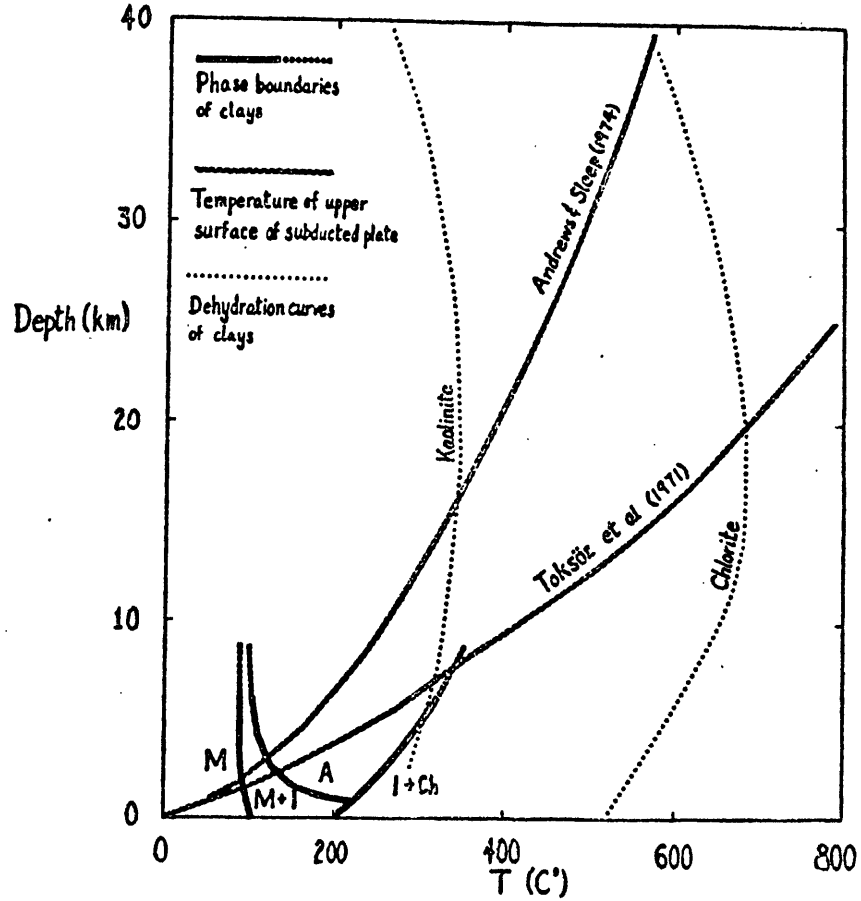

Figure 2

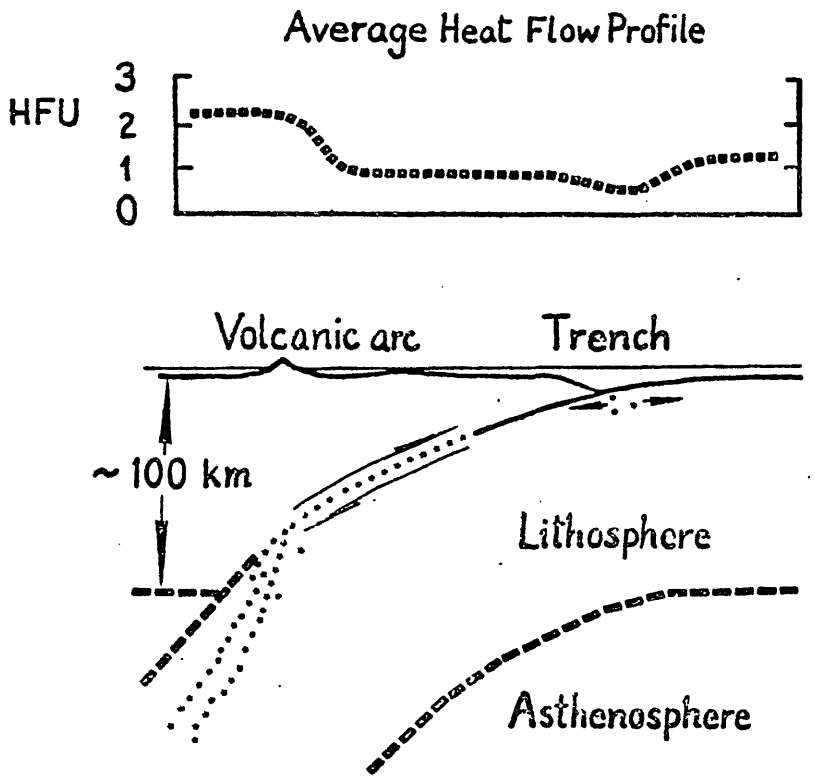
Average Heat Flow Profile
HFU
3
2
1
0
Volcanic arc
Trench
~ 100 km
Lithosphere
Asthenosphere

Figure 3

Chi-yuen Wang and Nai-hsien Mao[1]

Department of Geology and Geophysics, University of California, Berkeley, California 94720

Francis T. Wu

Department of Geological Sciences, State University of New York, Binghamton, New York 1390

Abstract. The mechanical properties of preconsolidated clays are studied at high pressures under undrained, triaxial conditions. At confining pressures equivalent to those at midcrust, different clays have the following common characteristics which differ significantly from those at low pressures: (1) the clays possess significant strength of several hundred bars (10 bars = 1 MPa); (2) the constitutive relations are marked by ductile yielding and strain hardening, followed by a broad peak strength and a gradual decrease in strength at greater deformation; and (3) the change in volume during shearing is small. On the other hand, the behavior of montmorillonite differs from that of the other clays (illite, chlorite, and kaolinite) in the following ways: (1) its peak strength at a given confining pressure is about half of the strengths of the other clays; (2) its peak strength occurs at a shortening of about 10%, while for the illite and chlorite the peak strength occurs at a shortening of 20-25% (for kaolinite, strain hardening continues even at 30% shortening); and (3) the fracture surfaces of some montmorillonite samples deformed at relatively low confining pressures show features resembling those in natural clayey fault gouge, whereas at higher confining pressures, montmorillonite and the other clays remain unfractured at shortening up to 30-40%.

Introduction

Laboratory experiments on frictional sliding [Byerlee, 1978] showed that the shear stress required to initiate rock-on-rock sliding at pressures equivalent to those at midcrustal depth is of the order of several kilobars. In situ stress measurement along the San Andreas fault [Zoback and Roller, 1979] and other active tectonic areas, on the other hand, has indicated a low shear stress. The absence of a clear anomaly in heat flow across the San Andreas fault was

[1]Permanent affiliation: Lawrence Livermore Laboratory, Livermore, California 94550

fault of no more than 200 bars [Brune et al., 1969].

Stesky and Brace [1973] showed that the large difference between the shear stress required to initiate rock-on-rock sliding and the shear stress on the San Andreas fault as estimated from heat flow cannot be explained by the effect of temperature or the fractured character of rocks in the fault zone; they suggested that the presence of low-strength alteration materials or high pore pressure in the fault zone may provide an adequate explanation.

It is known from surface exposure that fault gouge of various compositions occurs along active faults. Frequently, the gouge contains significant amounts of clay. Clay has also been found on faults in deep tunnels [e.g., Brekke and Howard, 1973] and in deep boreholes.

Experimental studies by clay mineralogists [e.g., Velde, 1969] have shown that montmorillonite and kaolinite form a stable mineral assemblage at pressures up to 3.5 kbar and temperatures up to 420°C. A recent interpretation of the seismic velocity and gravity across the San Andreas fault [Wang et al., 1978] showed that the geophysical data are also compatible with the hypothesis that large quantities of fault gouge may be present at depths down to 10 km.

If clay minerals are indeed present in large quantities at midcrustal depths along active faults, their mechanical properties would determine the behavior of faults. Laboratory experiments by Summers and Byerlee [1977] and Logan and Shimamoto [1976] have already shown that the characteristics of sliding between rocks is strongly modified by the presence of artificial gouge sandwiched between the sliding blocks. Summers and Byerlee [1977] and Byerlee [1978] showed that when the sliding surfaces are separated by a layer of clay of montmorillonite or vermiculite, the frictional resistance to sliding becomes very low.

Most of the previous experimental works pertaining to the mechanical properties of clays were done by soil mechanics researchers. As a consequence the data in the existing literature were obtained under very low confining pressures of a few bars [e.g., Lambe and Whitman, 1969; Mitchell, 1976], although a few experiments were performed under moderate pressures up to 70 bars [Olson and Parola, 1967]. At low confining pressure, clay exhibits little strength. But does clay stay virtually without strength at high confining pressure? If not, what is its strength at pressures at midcrustal depths, and how does the strength vary with pressure? If fault zones do contain large quantities of clayey gouge, how would the strength of a fault be determined

Based upon the low-pressure experimental data for granular material under shear deformation, Stuart [1974] proposed a qualitative model for the constitutive relation for fault gouge. The material exhibits strain hardening and attains a peak strength under sustained shearing and, on further deformation, gradually weakens to a residual strength. On the grounds of low-pressure soil mechanics data, Bombolakis et al. [1978] argued that such a qualitative model may also be applicable to silt-clay fault gouge. But does clayey gouge under midcrust conditions behave in much the same way? Experimental data for clays at high pressure may provide some insight to these questions.

In this work we investigate the mechanical strength of normally consolidated clays at confining pressures of 1-4 kbar under undrained, triaxial conditions. The effect of temperature and the effect of strain rate are no doubt of great importance in determining the strength of clays, but they will not be discussed in this paper.

In a preliminary note [Wang et al., 1979] we showed some experimental results for montmorillonite. This paper gives a full account of our results for four different clays, including montmorillonite, illite, chlorite, and kaolinite.

Sample Preparation

The clays used in the present study were 'API standard' clays, purchased from Wards. The samples came either in powder form or in solid blocks; the blocks were then crushed into powder. Microscopic study of the clay powder showed that most grains were less than 1 μm in diameter. Large grains of aggregates and single crystals up to 250 μm in diameter, on the other hand, were abundant and were probably dominant in terms of their relative volume. The various powdered clays were then sieved through standard sieves, so that clays of known grain sizes were obtained for preparing test samples.

A thin flexible membrane was filled with clay powder. Partial vacuum was then applied to the clay to remove most of the air. The membrane was then sealed and was placed in a high-pressure vessel, where it was hydrostatically compressed under an ambient pressure of 1-2.5 kbar for at least 20 hours.

For a given kind of clay the density of a consolidated sample appeared to depend upon the length of time that the sample was subjected to hydrostatic compression. Figure 1 shows the densities of the clays, preconsolidated at 2 kbar, as a function of consolidation time. Between 20 and 50 hours the density of montmorillonite

kaolinite the rate of density increase was about 0.1% and 0.03%, respectively. Table 1 lists the grain sizes, the confining pressures, the durations of consolidation, and the densities of the consolidated clays used in this investigation. No systematic dependence of density on grain size is obvious from this set of data. Also listed is the porosity of each clay sample, calculated from the density of the sample and its 'grain density' [Lambe and Whitman, 1969].

Before consolidation the clay powder had been exposed to room moisture for intervals from a few months to a year and presumably had reached an equilibrium with the ambient moisture. The amount of moisture in each clay is determined by weighing a fixed amount of clay powder before and after drying at 105°C for 2 weeks. The amount of moisture so determined, in weight percent, was 5–7% for montmorillonite, 0.7% for illite, 0.6% for chlorite, and 0.9% for kaolinite.

The consolidated samples were examined for any preferred orientation of the clay particles by using X ray diffraction techniques (the Meade technique and the pole density technique). No preferred orientation was detected for montmorillonite, illite, or kaolinite. A weak preferred orientation of grains was found in the consolidated chlorite sample, with the basal planes of the grains preferentially oriented perpendicular to the axis of the cylinder.

The consolidated clay specimens were machined into right cylinders (usually 6.3 cm in length and 2.5 cm in diameter) for the triaxial test. The middle sections of the cylindrical samples were coated with a thin film of liquid polyurethane, where four foil strain gages were later mounted. Two brass discs were placed on the ends of the sample. The entire assemblage was then covered with three layers of liquid rubber before the triaxial test. The rubber jacket was cut open after each test in order to detect any possible leakage. For the amount of strains in our experiments (up to 40% of shortening) the rubber jacket appeared to be very dependable.

Experimental Details

Experiments were carried out in a conventional triaxial apparatus, with fluid confining medium and an internal load cell for monitoring the axial force. Confining pressure was measured with a manganin cell and a Heise gage to 1% accuracy. Deformation of the specimen was measured by using two pairs of foil strain gages mounted on the middle section of the sample. Axial shortening of the samples was also measured by the use of a displacement transducer (DCDT) mounted

ment, both sets of deformation measurements recorded to provide independent checks.

A 10-channel signal conditioner (Vishay-2100) was used to amplify the signals from the strain gages and the manganin cell. The outputs of the conditioner and the DCDT were digitized via a 10-bit analog/digital converter and recorded on a magnetic disk in a PDP 11-10 minicomputer. The digitized data were displayed simultaneously on a Tektronix graphic terminal for on-line monitor. The sampling rate was typically set at 0.2 Hz. After each experiment the recorded data were processed and the important results were plotted on graph paper using an XY plotter.

Changes in sample dimensions due to hydrostatic and axial compression were calculated by using the strain gage data. Corrections to stress due to the changes in sample cross section were made in all stress calculations.

All experiments were carried out at room temperature. For montmorillonite, 10 experiments were carried out at confining pressures betwen 1 and 4 kbar. Two experiments were done on kaolinite, two on illite, and one on chlorite, all at 2 kbar confining pressure.

Experimental Results

Figure 2 shows a real-time record for a typical triaxial experiment. Hydrostatic pressure was raised to a level equal to the preconsolidation pressure and maintained at that level throughout the experiment. Note that when the pressure was increased, both the axial and the lateral strain gages showed an increase in strain (compression is taken to be positive). The rate of displacement was kept at a constant rate of 2.7×10^{-3} mm/s. For a sample of 6.25 cm in length this rate of displacement corresponds to a strain rate of 4×10^{-5} per second. In contrast to the pronounced axial and lateral strains during this phase of deformation the volumetric strain changed very little. Deformation was usually continued until the allowable displacement of the piston was used up.

Montmorillonite

The compression of the preconsolidated montmorillonite as a function of the hydrostatic pressure is shown in Figure 3. The axial and lateral strains were closely similar up to the maximum pressure, indicating that the sample was grossly isotropic. Up to 2 kbar the changes in strains with respect to pressure were relatively large as compared with those at higher pressure. At about 2 kbar there was a change in the slope of the curves, as is most evident

the slope of the strain versus pressure curves were also evident for the other montmorillonite samples and thus appear to be an intrinsic property of the material. We shall delay the discussion of this observation until a later section.

Figure 4 shows some examples of the stress-strain relations for two samples of montmorillonite: one determined at a confining pressure of 1.35 kbar and the other at 3.8 kbar. For both cases the maximum shear stress rose steeply in proportion to strain in the first 1-2% of the deformation. At greater deformation the rate of increase became gradually smaller. The curves gradually flattened out to reach a broad peak at an axial strain of 7-10% (or lateral strain of 4-5%). At greater deformation the strength of the clay began to decrease. For the case of the lower confining pressure (1.35 kbar) a relatively rapid decrease of the maximum shear stress of about 30 bars occurred at an axial strain of 13% (or lateral strain of 6%). Thereafter the strain gages registered no further changes in strain even though the piston was still advancing, as was indicated by the axial shortening of the sample. The curves for the axial shortening and the axial strain were remarkably consistent up to this event. The sample was probably fractured at this point, and beyond this point the displacement curve probably represented sliding in the fractured sample along some newly formed surface of discontinuity. The recovered sample was indeed fractured. The fracture surfaces were at an angle of about 30° to the axis of the sample; sliding on these surfaces was indicated by many slickenside marks and a higher degree of luster. Scanning electron microscopic study of the fracture surfaces suggested that the luster of the fracture surfaces may be a result of alignment of the clay platelets parallel to the fracture surface. These fine features resemble those observed in natural clayey fault gouge exposed on the earth's surface.

For the case at P = 3.8 kbar the maximum shear stress decreased gradually from its maximum value with increasing deformation up to the maximum axial shortening of 25%. The recovered sample was still in one piece, though it was crisscrossed by numerous fine cracks at angles of about 45° to the maximum principal stress axes. The total amount of decrease in the maximum shear stress in this case was about twice the amount that occurred at the lower pressure. Beyond 13% of shortening the maximum shear stress remained more of less constant.

For both samples of montmorillonite the volumetric strain changed little under deviatoric stresses until the peak strength was closely approached. For the case at P = 1.35 kbar,

volume decreased slightly with increasing shear. Close to the peak strength the sample showed a tendency to dilate, but the amount of dilation remained small. This characteristic for the change in the volumetric strain under deviatoric stress appeared to be common for the other montmorillonite clays tested at confining pressure below 2 kbar. At the confining pressure of 3.8 kbar the situation was quite different. With increasing deviatoric stress up to 90% of the peak strength the volume of the sample remained virtually constant. However, at higher deviatoric stresses the sample began to dilate, and after the peak strength was reached, the sample dilated rapidly with further deformation. We shall interpret these differences in the next section.

Figure 5 summarizes the peak strength data for montmorillonite at various confining pressures between 1 and 4 kbar. At confining pressures up to 2 kbar the peak strength increased with pressure but stayed virtually constant at higher confining pressures. Interpretation of this result is also deferred to the next section.

Kaolinite

Figure 6 shows the stress-strain relations for two kaolinites, both tested at a confining pressure of 2 kbar. The results for the two experiments were closely similar, even at large strains. The most striking differences between kaolinite and montmorillonite in terms of their mechanical properties are that (1) kaolinite continued to strain-harden even at an axial shortening of 30%, while montmorillonite reached a peak strength at an axial strain of about 10% and weakened thereafter, and (2) the strength of kaolinite was at least twice that of montmorillonite. Volumetric strain for kaolinite was again small; volume first decreased slightly and started to dilate at a stress difference of about 1 kbar. Up to the maximum deformation the axial strains determined from the foil strain gages were in close agreement with the axial strains determined from the displacement gage.

Chlorite

The stress-strain relations for chlorite, again determined at a confining pressure of 2 kbar, are given in Figure 7. The maximum shear stress reached a value of 660 bars at an axial shortening of 20%. A significant softening occurred at greater deformation. The volume of the sample decreased slightly with increasing shearing until the peak strength was closely approached, and thereafter the sample dilated with further deformation.

Two samples of illite were tested, both at a confining pressure of 2 kbar (Figure 8). For both samples the strain gages were not mounted correctly, and the only information for deformation was from the DCDT displacement data. A broad peak strength of about 800 bars occurred at about 25% strain, and the samples gradually softened at greater strains. Note the remarkable similarity between the two experimental results, indicating the repeatability of our experiments.

The recovered chlorite and illite samples after shearing were crisscrossed by numerous fine cracks oriented at about 45° to the axes of the samples. Examination with a microscope showed that these cracks appeared as sharp discontinuities in the samples and that across these cracks much displacement had apparently taken place. On the other hand, no cracks were found on the surfaces of the deformed kaolinite samples.

Discussion

Comparison With Previous Studies

Summers and Byerlee [1977] and Byerlee [1978] showed that when rock joints are filled with montmorillonite or vermiculite, the frictional resistance to sliding becomes very low. Their data showed that at a confining pressure of 3.6 kbar, rock joints filled with montmorillonite clay have a shear strength of 0.7 kbar; higher strength was indicated for higher confining pressures. The present study shows that the strength of the montmorillonite clay under equivalent confining pressures is lower than the clay-filled joint. Part of this difference might be due to the undrained condition in our experiment, so that pore pressure might have built up in our samples at confining pressures greater than 2 kbar (see the next section for an explanation). It is conceivable that in the experiments of Summers and Byerlee the clay wafers between the rocks were under a drained condition, where water could escape from the clay to the pores of the rock. If this assumption is correct and if the strain rate in the experiment of Summers and Byerlee was small enough to allow diffusion of water to the pores of the rock, the higher strength of the clay wafers is expected.

Another possible explanation for the different results may lie in the testing techniques: while Summers and Byerlee sheared thin layers of clays between rock pieces, we sheared whole clay samples under triaxial conditions. Byerlee et al. [1978], Engelder et al. [1976], and C.Y. Wang (unpublished results, 1979) found that in the sliding experiments, much sliding took place

the sliding rock. It seems reasonable to conjecture that the sliding behavior in these experiments was significantly influenced by the interaction between the clay and the rock at their boundaries, rather than solely determined by the mechanical property of the clay. Thus a direct comparison of the results from the sliding experiments with those of the present study may not be meaningful. On the other hand, it is interesting to note that the stronger clays, like kaolinite, illite, and chlorite, induced higher frictional resistance and even violent stickslips in the sliding experiments, while the weak, claylike montmorillonite induced only weak frictional resistance without any sudden releases of stress [Summers and Byerlee, 1977].

On the Strength of Montmorillonite

A remarkable feature in Figure 5a is that the peak strength of montmorillonite stayed virtually constant at confining pressures of about 2 kbar. This might be due to pore pressure built up in the sample at confining pressures greater than 2 kbar, so that the effective confining pressure remained constant. There are two lines of evidence which indicate that the montmorillonite samples became saturated at a confining pressure of about 2 kbar. First, the compression curves for montmorillonite (e.g., Figure 3) all showed abrupt changes in slope at a confining pressure of about 2 kbar. The samples were much more compressible below this pressure. The volumetric compressibility for the montmorillonite sample changed from 0.03 to 0.007 per kilobar across the transition. The volumetric strain at which this change occurred was about 12%. Comparing this value with the previous estimated porosity in the sample (Table 1) and making the reasonable assumption that up to 2 kbar much of the decrease in volume was due to the elimination of empty pores, we may interpret the abrupt change in the slopes of the compression curves as being due to saturation of the sample at this pressure. Since the sample was under an undrained condition, pore pressure might have built up in the sample at higher confining pressures. Dropek et al [1978] reported similar changes of compressibility of a sandstone when it was compressed to saturation.

Another line of evidence comes from the change of sample volume during shearing, and this bears a more subtle relation to the degree of saturation in the sample. The curves for volumetric strains in Figure 4 show that at low confining pressure, shearing caused a small but clear decrease in the volume of the sample. As was pointed out by Brace [1978], such decrease

of porous rocks and is probably related to the collapse of empty pores in the sample during shearing. At the high confining pressure of 3.8 kbar, on the other hand, shearing was no longer associated with a decrease in the sample volume; the volumetric strain remained negligible during shearing until the sample was sheared close to its peak strength, where dilatancy commenced. This constancy in volume during shearing might be related to pore pressure buildup which resisted further compaction of the sample.

The moisture in the other clays (Table 1) was less than 1% by weight; thus the decrease in pore volume under a confining pressure of 2 kbar was probably insufficient to eliminate all the empty pores; i.e., the clays probably remained undersaturated at 2 kbar. During shearing, both kaolinite (Figure 6) and chlorite (Figure 7) showed a decrease in volume until the samples began to dilate; these decreases in volume may also have been related to the collapse of empty pores.

On the Mechanism for the Postpeak Softening of Consolidated Clays

It is well known from low-pressure soil mechanical experiments that when subjected to repeated shearing, most clays develop a lower and lower angle of internal friction, i.e., are more and more prone to slippage. This happens when the interlocking grains are rearranged so that the scalelike and flake-shaped clay particles adjust themselves toward the shear plane until they form a continuous, shiny shear surface (slickensided clays [e.g., Borowicka, 1965]). It is tempting to associate this mechanism with the phenomenon of strain softening in compacted clays under high confining pressures as observed in the present study. In this model, the peak strength of clays may indicate the shear stress necessary to overcome the resistance between the interlocking grains to rearrange themselves toward a common shear plane. Because of its lower strength, subsequent fault motion tends to occur along this common shear plane. This effect tends to delineate the slip planes, which after the occurrence of extensive slippage, show up as the multitude of fine cracks which are observed on the recovered samples. It is interesting to note that the recovered kaolinite samples which did not show strain softening displayed no visible cracks on their surfaces.

Implications for Fault Movement

There are several difficulties in applying the experimental results to the study of fault movement. On natural faults, most gouge

materials are complex mixtures of rock fragments and clays in various proportions. The differences between the mechanical behavior of such mixtures and that of compacted pure clays are not clear at this moment. Furthermore, the strain rate for our experiments is probably many orders of magnitude greater than that which occurs along active faults. No reliable extrapolation of the experimental results to the field situation may be made without an understanding of the loading rate effect. On the other hand, even in the absence of such understanding, some inferences on fault movement may still be drawn from the present experimental study.

A common characteristic in the mechanical property of consolidated clays under high confining pressure and prolonged shearing is the occurrence of a peak strength and a postpeak decrease in strength to reach a lower residual strength. The same qualitative characteristic is also present in the mechanical properties of over-consolidated clays and densely packed brittle granular materials [Lambe and Whitman, 1969]. It seems quite probable for fault gouges, which are densely packed mixtures of various clays and rock fragments, that such general characteristics may also be true. The effect of this postpeak decrease in strength may be important in generating instabilities in the fault zone [Stuart, 1974].

Acknowledgments. We thank Tom Dey, Ivy Kuo, and David Auslander for providing computer programs used in this study for data assemblage and graphic display. Len Vigus maintained the high pressure equipment and George Engeman assisted in interfacing some of the electronic components used in this experiment. This research was supported by a USGS grant, USDI-14-08-0001-17747.

References

Bombolakis, E. G., J. C. Hepburn, and D. C. Roy, Fault creep and stress drops in saturated silt-clay gouge, J. Geophys. Res., 83, 818, 1978.

Borowicka, H., The influence of colloidal content on the shear strength of clay, Int. Conf. Soil Mech. Foud. Eng. 6th, 1, 175, 1965.

Brace, W. F., Volume changes during fracture and frictional sliding: a review, Pure Appl. Geophys., 116, 603, 1978.

Brekke, T. L., and T. R. Howard, Functional classification of gouge materials from seams and faults in relation to stability problems in underground openings, final report, Dep. of Civil Eng., Univ. of Calif., Berkeley, 1973.

Brune, J. N., T. L. Henyey, and R. F. Roy, Heat flow and rate of slip along the San Andreas fault, California, J. Geophys. Res., 74, 3821, 1969.

phys., 116, 615, 1978.
Byerlee, J., V. Mjachkin, R. Summers, and D. Voevoda, Structures developed in fault gouge during stable sliding and stick-slip, Tectonophysics, 44, 161, 1978.
Dropek, R. K., J. N. Johnson, and J. B. Walsh, The influence of pore pressure on the mechanical properties of Kayenta sandstone, J. Geophys. Res., 83, 2817, 1978.
Engelder, J. T., J. M. Logan, and J. Handin, The sliding characteristics of sandstone on quartz fault-gouge, Pure Appl. Geophys., 113, 68, 1975.
Lambe, T. W., and R. V. Whitman, Soil Mechanics, 553 pp., John Wiley, New York, 1969.
Logan, J., and T. Shimamoto, The influence of calcite gouge on frictional sliding of Tennessee sandstone (abstract), Eos Trans. AGU, 57, 1011, 1976.
Mitchell, J. K., Fundamentals of Soil Behavior, 422 pp., John Wiley, New York, 1976.
Olson, R. E., and J. F. Parola, Dynamic shearing properties of compacted clay, in International Symposium on Wave Propagation and Dynamic Properties of Earth Material, pp. 173-182, University of New Mexico Press, Albuquerque, New Mexico, 1967.
Stesky, R. M., and W. F. Brace, Estimation of frictional stress on the San Andreas fault from laboratory experiments, in Proceedings of the Conference on Tectonic Problems of the San Andreas Fault System, pp. 206-214, Stanford University Press, Stanford, Calif., 1973.
Stuart, W. D., Diffusionless dilatancy model for earthquake precursors, Geophys. Res. Lett., 1, 261, 1974.
Summers, R., and J. Byerlee, A note on the effect of fault gouge composition on the stability of frictional sliding, Int. J. Rock Mech. Miner. Sci., 14, 155, 1977.
Velde, B., The compositional join muscovite-pyrophyllite at moderate temperature and pressure, Bull. Soc. Fr. Mineral Cristallogr., 92, 360, 1969.
Wang, C. Y., W. Lin, and F. T. Wu, Constitution of the San Andreas fault zone at depth, Geophys. Res. Lett., 5, 741, 1978.
Wang, C. Y., N. H. Mao, and F. T. Wu, The mechanical property of montmorillonite clay at high pressure and implications on fault behavior, Geophys. Res. Lett., 6, 476, 1979.
Zoback, M. D., and J. C. Roller, Magnitude of shear stress on the San Andreas fault: implications of a stress measurement profile at shallow depth, Science, 206, 445, 1979.

(Received April 27, 1979;
revised December 5, 1979;
accepted December 20, 1979.)

TABLE 1. Specifications of Clay Samples

Sample Number	Type of Clay	Before Consolidation	Consolidation		After Consolidation	
		Grain Size μm	Pressure kbar	Time hours	Density g/cm^3	Porosity %
2	montmorillonite (Wyoming)	<60	2.0	66	2.196	19.9
3	kaolinite (Georgia)	<120	2.0	24	2.123	18.7
7	montmorillonite (Wyoming)	<60	2.0	21	2.166	20.9
9	montmorillonite (Wyoming)	<60	2.0	24	2.167	20.9
10	illite (New York)	<60	2.0	23	2.212	18.8
11	montmorillonite (Wyoming)	<180	2.0	72	2.215	19.2
13	kaolinite (Georgia)	<120	2.0	24	2.118	18.8
25	illite (New York)	<60	2.0	50	2.233	18.0
26	montmorillonite (Wyoming)	<60	2.0	48	2.193	20.0
40	montmorillonite (Wyoming)	<60	1.0	46		
52	montmorillonite (Wyoming)	<180	2.5	64	2.220	19.2
53	montmorillonite (Wyoming)	<60	1.0	70	2.100	21.9
57	montmorillonite (Wyoming)	<60	1.0	88	2.164	20.9

Porosity is calculated according to $n \approx 1 - d/d'$, where d is the density of the sample and d' is the density of the clay particles [Lambe and Whitman, 1969].

2 kbar, as a function of consolidation time.

Fig. 2. A real-time record for a typical triaxial test: ε_z, ε_θ, and ε_v are the axial strain, the lateral strain, and the volumetric strain, respectively; σ_z and σ_r are the axial stress and the confining pressure, respectively; u is the displacement of the piston.

Fig. 3. Strains of a montmorillonite sample under hydrostatic compression.

Fig. 4. Stress-strain relations for two montmorillonite samples under triaxial tests, one at a confining pressure of 1.35 kbar, the other at 3.8 kbar.

Fig. 5. Peak strength of montmorillonite as a function of confining pressure.

Fig. 6. Stress-strain relations for two kaolinite samples under triaxial tests, both at 2-kbar confining pressure.

Fig. 7. Stress-strain relations for a chlorite sample under triaxial test, at a confining pressure of 2 kbar.

Fig. 8. Stress-shortening relations for two illite samples in triaxial tests, both at 2-kbar confining pressure.

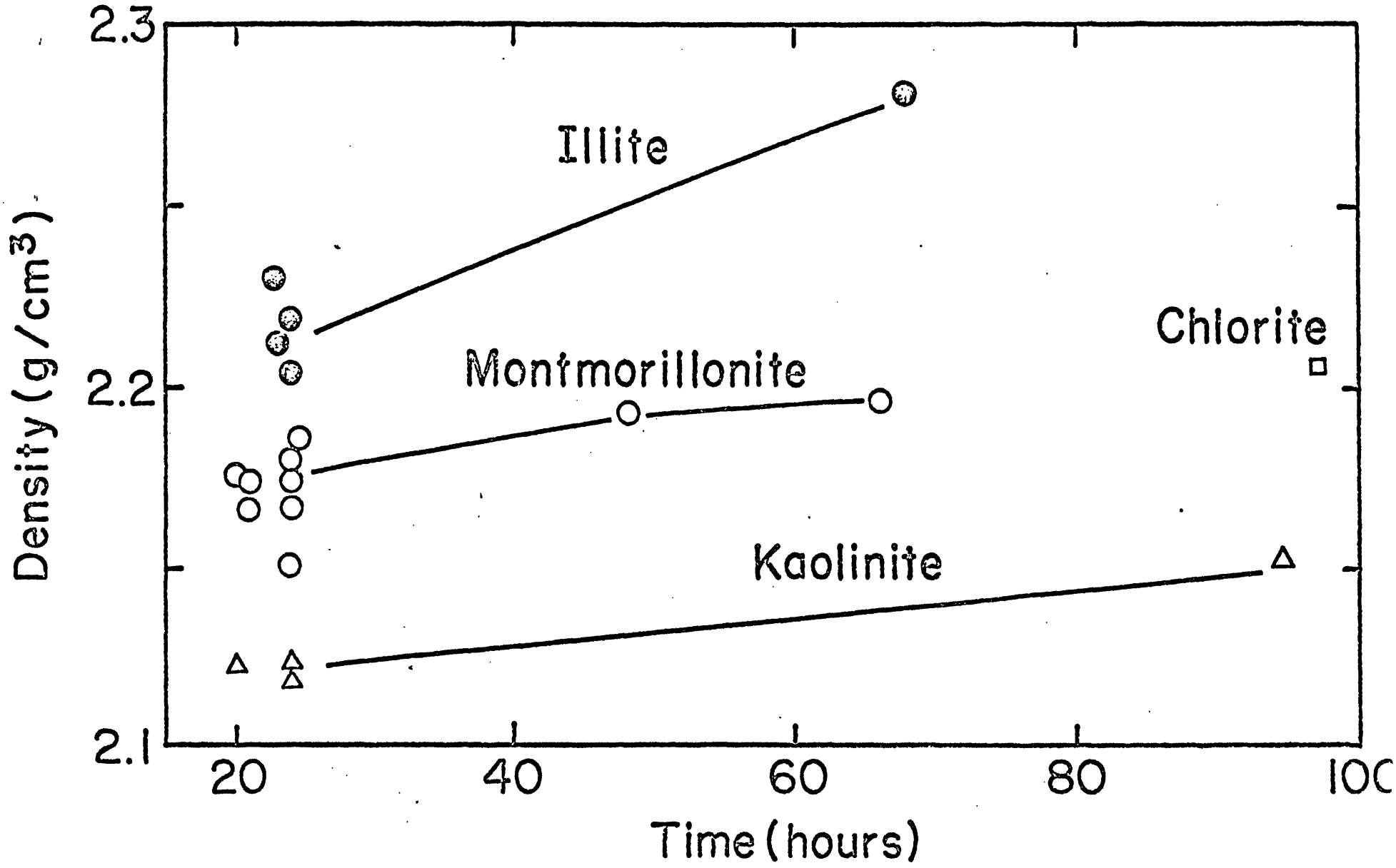
2.3
2.2
2.1
Density (g/cm³)
Illite
Montmorillonite
Chlorite
Kaolinite
20
40
60
80
100
Time (hours)

Fig. 1

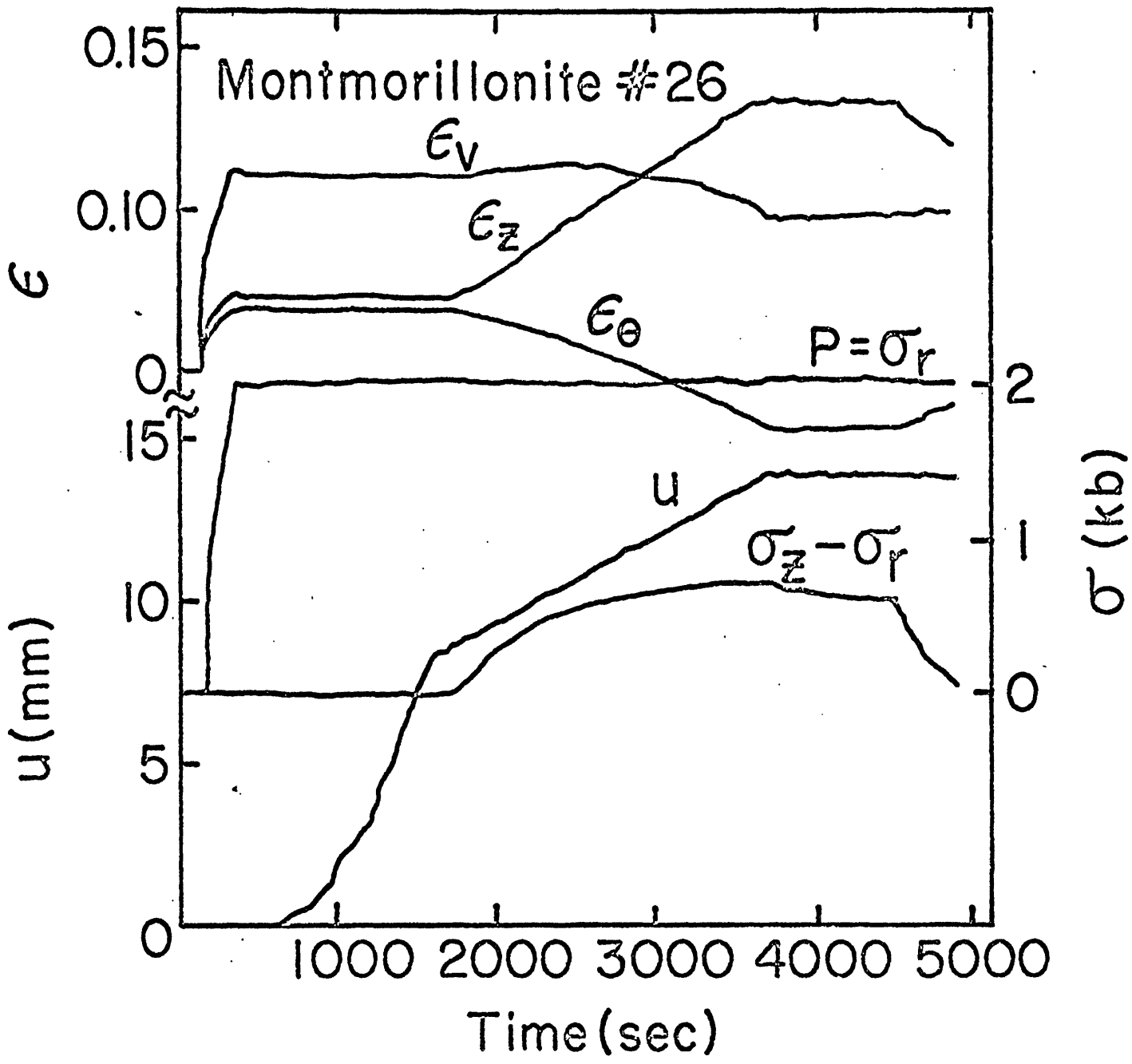
Montmorillonite #26
ϵ_v
ϵ_z
ϵ_θ
$P=\sigma_r$
u
$\sigma_z-\sigma_r$
ϵ
u(mm)
σ (kb)
Time (sec)
0.15
0.10
0
15
10
5
0
2
1
0
1000 2000 3000 4000 5000

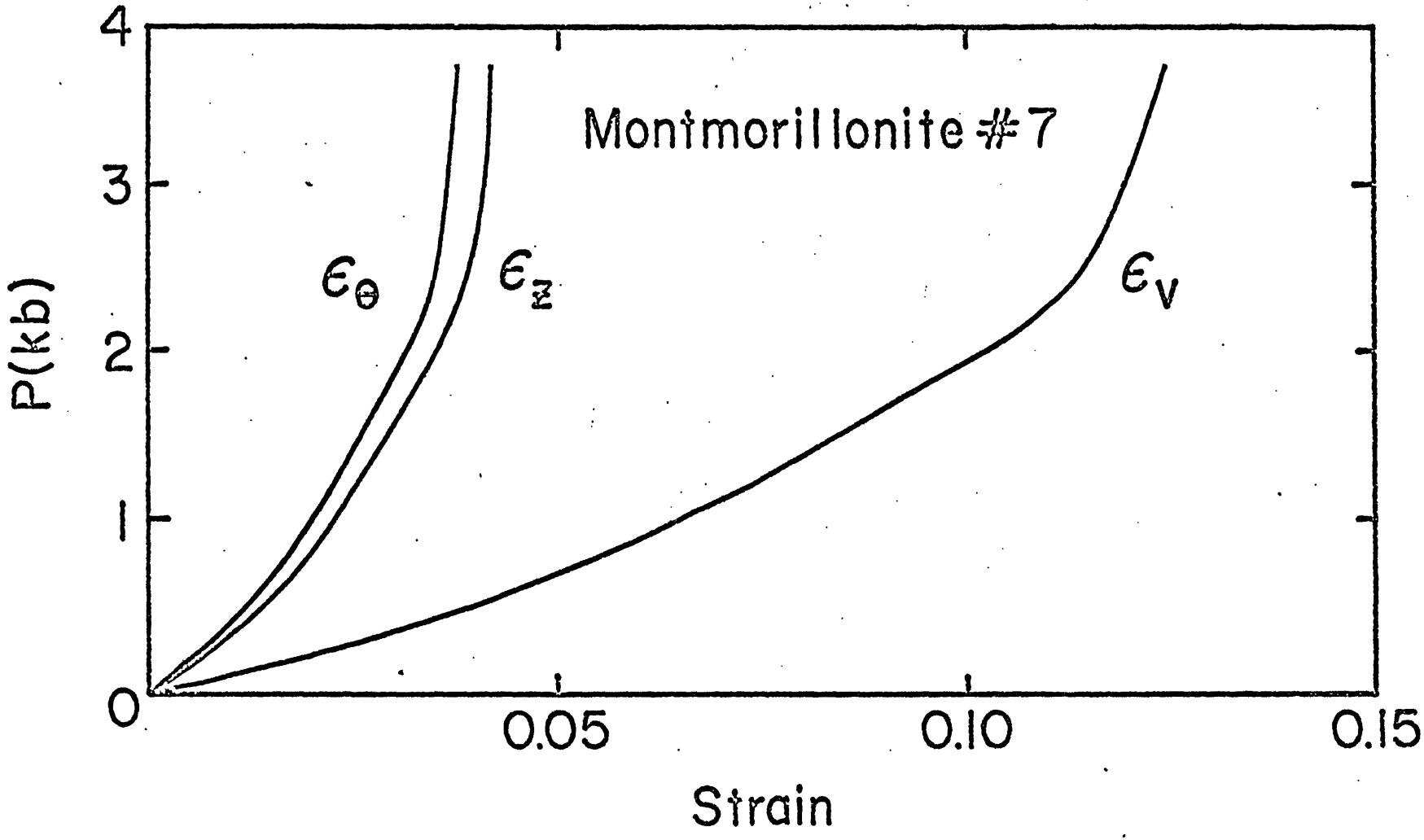
Montmorillonite #7
ϵ_θ
ϵ_z
ϵ_v
P(kb)
0
1
2
3
4
0.05
0.10
0.15
Strain

Fig. 3

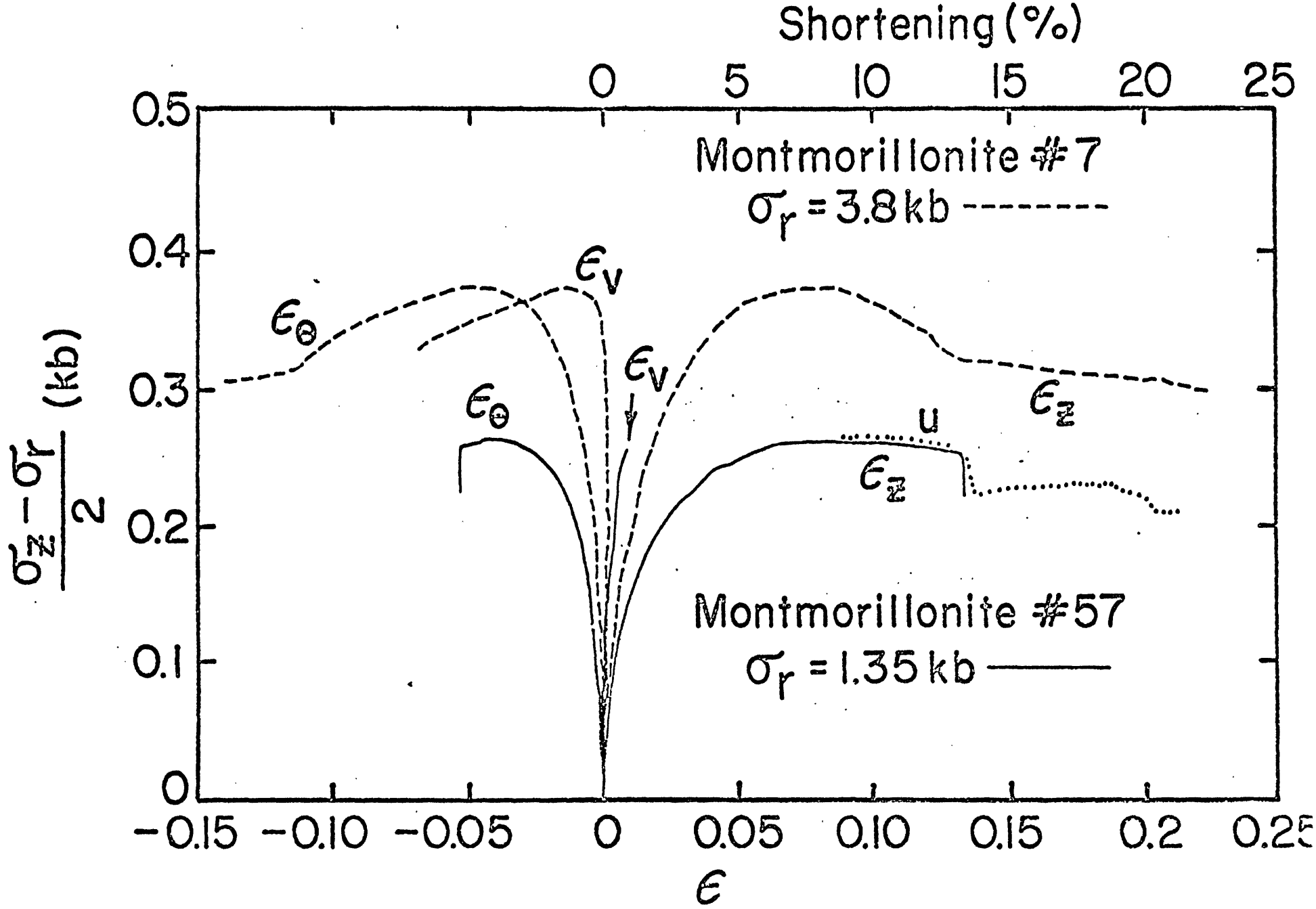
Shortening (%)
0
5
10
15
20
25
0.5
0.4
0.3
0.2
0.1
0
Montmorillonite #7
σ_r = 3.8 kb
ϵ_θ
ϵ_v
ϵ_v
ϵ_θ
ϵ_z
u
ϵ_z
Montmorillonite #57
σ_r = 1.35 kb
$\frac{\sigma_z - \sigma_r}{2}$ (kb)
−0.15
−0.10
−0.05
0
0.05
0.10
0.15
0.2
0.25
ϵ

Fig 4

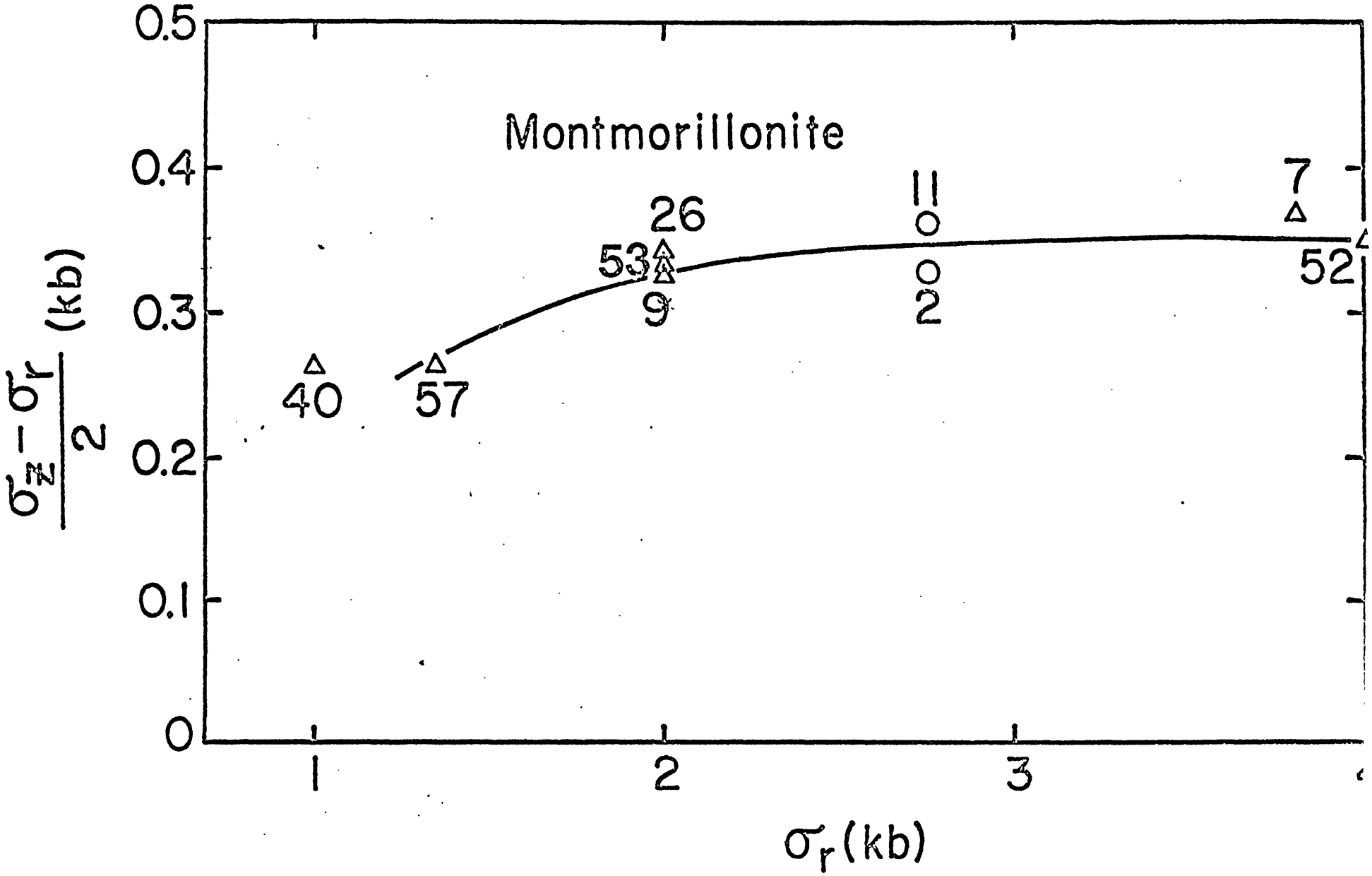
Montmorillonite
0.5
0.4
0.3
0.2
0.1
0
1
2
3
σ_r (kb)
$\frac{\sigma_z - \sigma_r}{2}$ (kb)
40
57
53
26
9
11
2
7
52

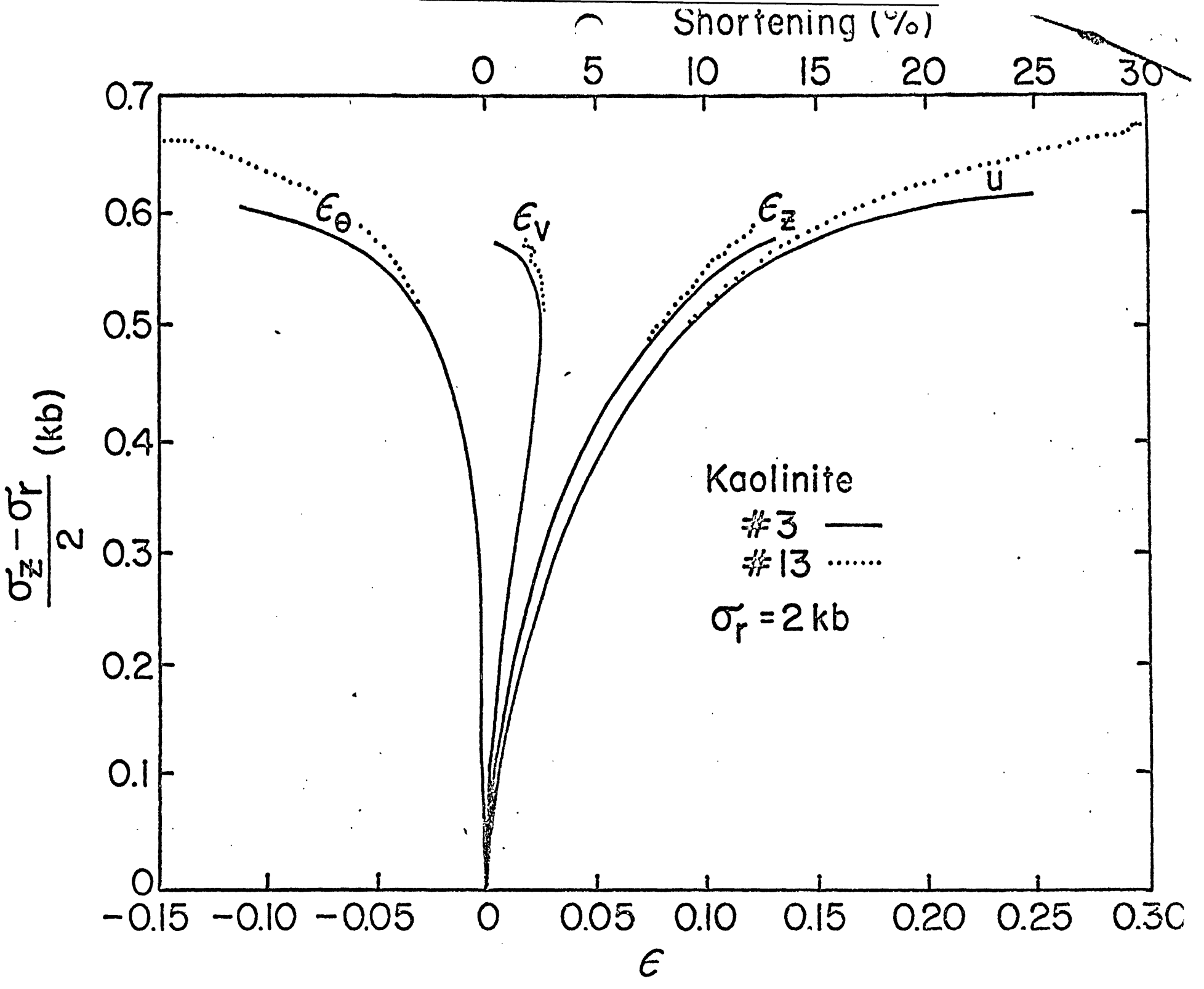
Shortening (%)
0
5
10
15
20
25
30
0.7
0.6
0.5
0.4
0.3
0.2
0.1
0
$\frac{\sigma_z - \sigma_r}{2}$ (kb)
ϵ_θ
ϵ_v
ϵ_z
u
Kaolinite
#3
#13
σ_r = 2 kb
−0.15
−0.10
−0.05
0
0.05
0.10
0.15
0.20
0.25
0.30
ϵ

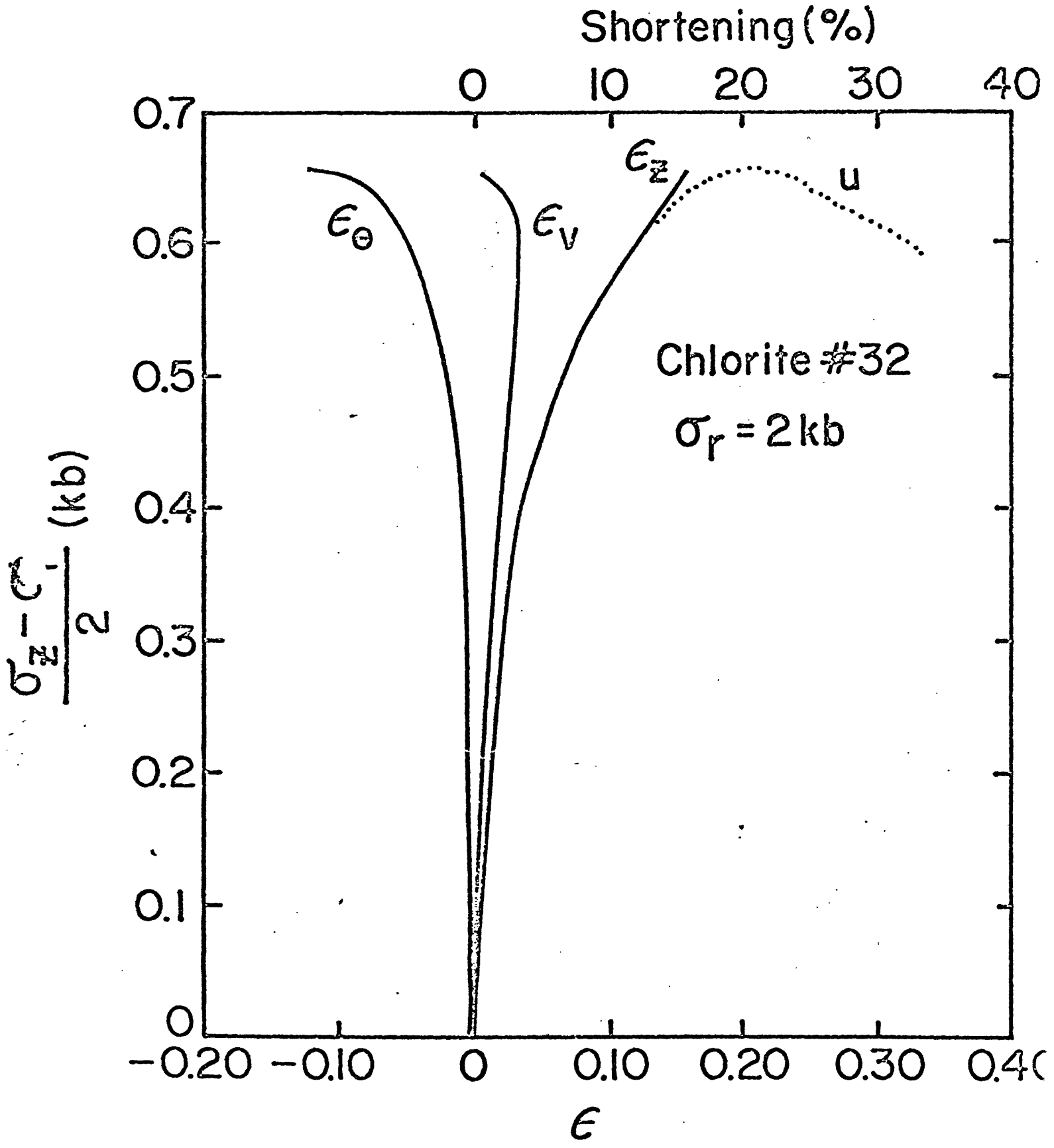
Shortening (%)
0
10
20
30
40
0.7
0.6
0.5
0.4
0.3
0.2
0.1
0
ϵ_θ
ϵ_v
ϵ_z
u
Chlorite #32
σ_r = 2 kb
$\frac{\sigma_z - \sigma_r}{2}$ (kb)
−0.20
−0.10
0
0.10
0.20
0.30
0.40
ϵ

Fig. 7

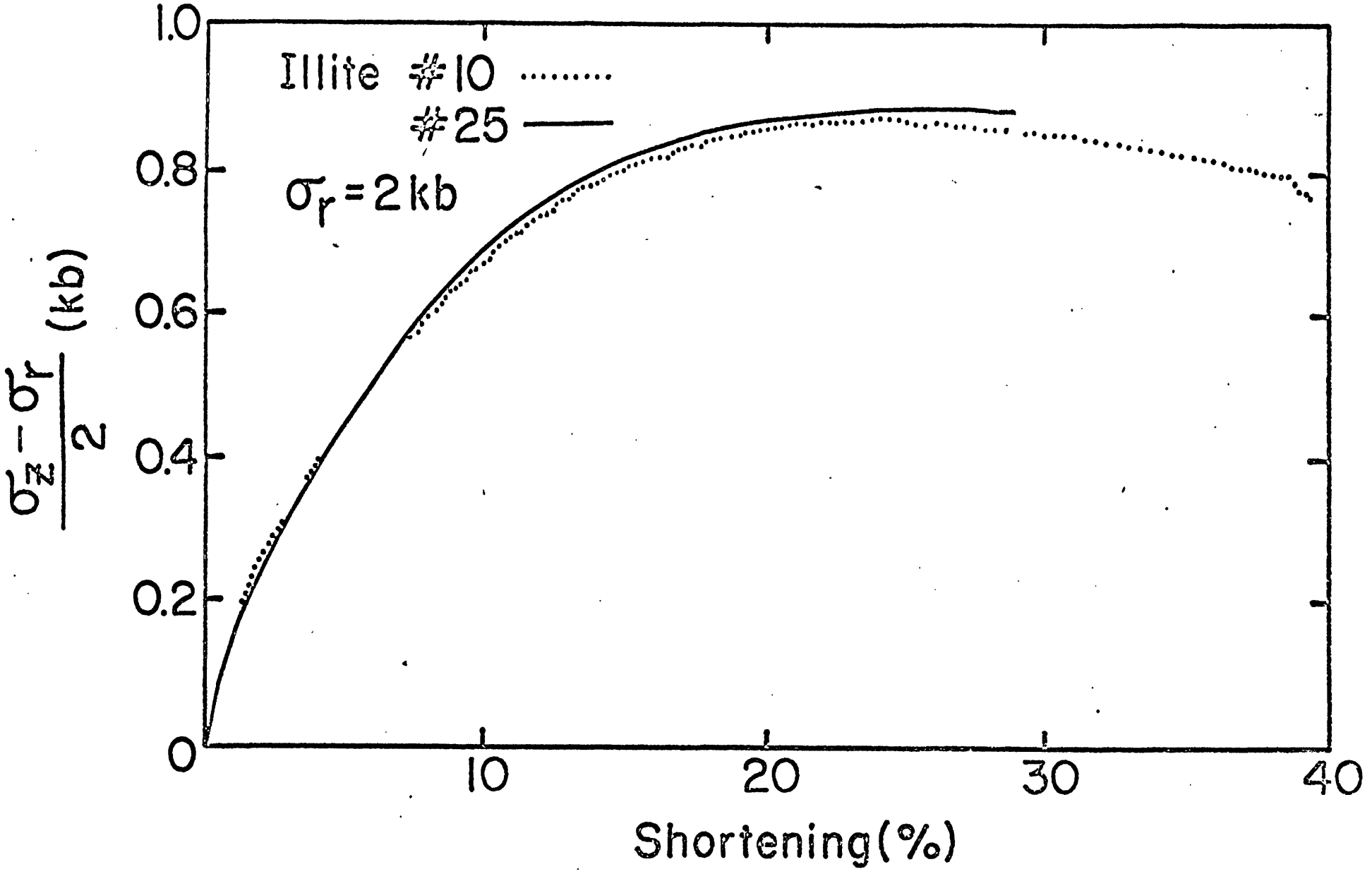
Illite #10
#25
σ_r = 2 kb
$\frac{\sigma_z - \sigma_r}{2}$ (kb)
1.0
0.8
0.6
0.4
0.2
0
10
20
30
40
Shortening (%)